Multi-species Lattice Boltzmann Models and Practical Examples

Short Course Material - An introduction to Lattice Boltzmann Methods for complex flow simulations - Rome 2008, Italy

Pietro Asinari, PhD

Department of Energetics, Politecnico di Torino

Corso Duca degli Abruzzi 24, Zip Code 10129, Torino, Italy

Tel. +39-011-090-4520, Fax. +39-011-090-4499

e-mail: *pietro.asinari@polito.it*, home page: *http://staff.polito.it/pietro.asinari*

March 5^{th}, 2008, Version 1.2

Contents

1 Introduction

1.1 Instructions for this document

Some suggestions on how to use this document are reported. For each section, it is important for the reader to understand the comments, which are highlighted as

(!!) important comments.

At the first reading, this allows one to skip the details of the mathematical derivations.

1.2 Useful definitions and applications

In order to understand which kind of applications will be discussed in this lecture, let us introduce first the following definitions.

Definition 1 (of species) *An ensemble of chemically identical molecular entities that can explore the same set of molecular energy levels on the time scale of the experiment.*

The first part of the previous definition is quite simple, i.e. a species is composed by chemically identical molecular entities. The second part is slightly more complicated. The latter part allows one to better clarify the attribute *identical* for some molecular entities. In fact, some molecular entities may show different properties with regards to a very fast perturbation, but, on the other hand, in a slow experiment the same mixture of entities may behave as a single chemical species, i.e. there is virtually complete equilibrium population of the total set of molecular energy levels belonging to the considered entities. This means that it is better to define some molecular entities as *identical* with regards to the perturbations and the time scales involved in the considered experiment.

(!!) It is worth the effort to point out that the definition of species only refers to the *chemical properties* of the considered entities, without any constraints to the *physical properties*.

Definition 2 (of phase) *A chemically and physically uniform quantity of matter that can be separated mechanically and it may consist of a single substance or of different substances.*

More precisely, a phase is a region in the parameter space of thermodynamic variables in which they are analytic. Between such regions there are abrupt changes in the properties of the system, which correspond to discontinuities in the thermodynamic variables and/or their derivatives.

Phases are sometimes confused with states of matter, but there are significant differences. States of matter refers to the differences between gases, liquids, solids, etc. If there are two regions in a chemical system that are in different states of matter, then they must be different phases. However, the reverse is not true because a system can have multiple phases which are in equilibrium with each other and also in the same state of matter.

Definition 3 (of mixture) *A system constituted by different species (multi-species mixture) and/or by different phases (multi-phase mixture).*

Definition 4 (of component) *A constituent element of a system and, in particular, one of the individual entities contributing to a whole mixture.*

The definition of *component* (and consequently the expression multi-component) is somehow ambiguous, because it is not immediately clear if it refers to a species (chemically identified entity) or a phase (both chemically and physically identified entity). However it always means that different entities are considered and hence it implies the existence of a mixture.

> (!!) Let us consider a multi-phase mixture. The definition of phase refers to both the chemical properties and the *physical properties* of the considered entities. Since the phases can be separated mechanically from the mixture, then *some level of separation* exists at a scale well above the molecular level. Consequently two phases can not strictly coexist in the same point.

Definition 5 (of the characteristic scale of separation δ_s) *Let us call $\partial\Omega^\sigma$ the interface between a generic phase σ and the other phases, which constitute the mixture. It is possible to define as δ_s^σ the characteristic length scale of the previous surface. Let us now consider the largest of these parameters, namely $\delta_s \geq \delta_s^\sigma$ for any phase σ. Actually this parameter can be generalized to any mixture, by assuming $\delta_s = 0$ by definition in case of a single-phase mixture.*

Let us now define as L the smallest characteristic length scale of the phenomenon. For example, this length scale can be imagined as the characteristic length, over which the spatial gradients of the flow variables show a meaningful variation. According to the previous definitions, the possible flows in a multi-phase mixture can be classified [1] as

- *disperse flows* $\delta_s \ll L$:
  - nearly homogeneous flow, it is the asymptotic limit of a disperse flow in which the disperse phase is distributed as an infinite number of infinitesimally small particles, bubbles, or drops and this limit implies zero relative motion between the phases;

  - bubbly or mist flow, it is a flow quite disperse in that the particle size is much smaller than the pipe dimensions but in which the relative motion between the phases is significant;

- *separated flows* $\delta_s \gg L$:
  - annular or film flow, it is a flow where the droplets are an important feature and therefore it can only be regarded as partially separated;
  - fully separated flow, it consists of two single phase streams when low velocity flow of gas and liquid in a pipe.

Any numerical modeling modifies the original set of characteristic scales of the phenomenon. Usually the actual smallest scale of the numerical description of the phenomenon differs from the smallest scale of the phenomenon itself. This is due to the fact that we introduce infinitesimal geometrical entities (mesh entities) in order to compute numerically the continuous operators. Let us define as δ_x the smallest characteristic length scale of our description of the phenomenon. For example, this length scale can be imagined as the discretization mesh size, used by a proper numerical scheme.

Definition 6 (of homogeneous mixture) *A generic mixture characterized by a characteristic length scale of separation δ_s which is much smaller than the size of the smallest scale of the description of the phenomenon, i.e. $\delta_s \ll \delta_x$ which means that, in case of multi-phase flows, the disperse phase particles (namely drops or bubbles) are much smaller than the smallest control volume of the description or, equivalently, each control volume contains representative samples of each of the phases.*

> (!!) The last definition allows the reader to understand the meaning of the title of this lecture. The key idea is that the following considerations can be applied to any (single- or multi-phase) multi-species mixture, if and only if each component is present (at least in very small quantities) in any control volume. Hence, for example, capillarity and interface-tracking problems are neglected.

The previous considerations apply also to the popular Continuous Phase Models (CPM) used for multi-phase flows by the scientific and engineering community [1].

Finally, the reactive flows are neglected in this lecture. Taking into account reactive flows by including reactive terms in the equations governing the single species dynamics seems a straightforward activity. However at least three difficulties arise.

- Most of the practical chemical models for reactive flows involve differential equations in order to compute the source terms and the minimum number of equations to be considered is usually very huge. For example, the meaningful skeleton set for methane-air combustion involves 25 reactions and 15 species, in order to properly take into account the leading bimolecular reactions, dissociations and recombinations.

- Most of chemical mechanisms can be modeled by means of reversed and effective reactions. The reaction rate is determinated by an equilibrium reaction constant, as defined by law of mass action. Unfortunately the last condition is highly non linear (not simply quadratic as it happens for the non linear terms in Navier-Stokes equations).

- Finally, in most of the cases, the previous chemical model is too complicated to be directly solved. For this reason, some systematic reduction techniques based on complex mathematical algorithms must be considered.

2 Macroscopic modeling

2.1 Concentration measures, mixture velocity and diffusion fluxes

Let us introduce some concentration measures in order to identify the relative composition of the mixture in a generic point [2]. In particular, the *mass* concentration is defined as

$$x_\sigma = \rho_\sigma / \rho, \tag{1}$$

where ρ_σ is the single species density [1], while $\rho = \sum_\varsigma \rho_\varsigma$ is the total mixture density.

Let us introduce the *molar* density as

$$n_\sigma = \rho_\sigma / m_\sigma, \tag{2}$$

where m_σ is the molecular weight, i.e. the weight of one mole of molecules. By means of the previous quantity is possible to define a *molar* concentration as

$$y_\sigma = n_\sigma / n, \tag{3}$$

where $n = \sum_\varsigma n_\varsigma$ is the total mixture *molar* density.

By means of the previous quantities, it is possible to define the relative fluxes describing the peculiar flow of each component of the mixture. In particular, by means of the *mass* concentrations, it is possible to define a *mass*-averaged mixture velocity, namely

$$\boldsymbol{u} = \sum_\varsigma x_\varsigma \boldsymbol{u}_\varsigma, \tag{4}$$

where $\boldsymbol{u}_\varsigma$ is the single species velocity. Since the *mass* concentrations where used, the previous quantity is also called *barycentric* velocity. Consequently it is possible to define a specific *mass* diffusion flux for each species σ as

$$\boldsymbol{j}_\sigma = \rho_\sigma \boldsymbol{w}_\sigma, \tag{5}$$

where $\boldsymbol{w}_\sigma = \boldsymbol{u}_\sigma - \boldsymbol{u}$ is the *mass* diffusion velocity and clearly $\sum_\varsigma \boldsymbol{j}_\varsigma = 0$.

Similarly, by means of the *molar* concentrations, it is possible to define a *mole*-averaged mixture velocity, namely

$$\boldsymbol{v} = \sum_\varsigma y_\varsigma \boldsymbol{u}_\varsigma. \tag{6}$$

Consequently it is possible to define a specific *molar* diffusion flux for each species σ as

$$\boldsymbol{k}_\sigma = n_\sigma \boldsymbol{z}_\sigma, \tag{7}$$

where $\boldsymbol{z}_\sigma = \boldsymbol{u}_\sigma - \boldsymbol{v}$ is the *molar* diffusion velocity and clearly $\sum_\varsigma \boldsymbol{k}_\varsigma = 0$.

[1] In case of multi-phase mixtures, ρ_σ is the apparent phase density, which is related to the actual one ρ'_σ by means of the generic volume fraction α_σ of the phase σ, i.e. $\rho_\sigma = \alpha_\sigma \rho'_\sigma$. This is due to the fact that $\rho_\sigma = M_\sigma / V$, while the actual phase density is $\rho'_\sigma = M_\sigma / V_\sigma$ and for multi-phase mixtures $\sum_\varsigma V_\varsigma = V$.

2.2 Species transport equation

Concerning multi-species flow modeling, it is not clear which mixture velocity is the best in order to describe the mixture dynamics. Actually the mixture literature would be a much deal simpler if there were only one way to characterize the mixture dynamics [2]. This has produced some ambiguities in defying the macroscopic transport equations (and the corresponding transport coefficients) for mixture modeling.

As far as the basic assumptions of the kinetic theory of gases are satisfied, it is always better to refer to the latter in order to deduce the macroscopic transport coefficients. However in this case, a popular alternative based on the equation of change of the species mass is proposed in order to start with an *heuristic* discussion of the macroscopic models [2].

Let us consider the Equation of Change for the species mass, which is a conserved quantity since the chemical reactions are neglected, namely

$$\frac{d}{dt}\int_{\Omega_\sigma}\rho_\sigma dV = \int_{\Omega_\sigma}\frac{\partial\rho_\sigma}{\partial t}dV + \int_{\partial\Omega_\sigma}(\rho_\sigma \boldsymbol{u}_\sigma)\cdot\boldsymbol{n}dS = 0, \tag{8}$$

and consequently

$$\frac{d}{dt}\int_{\Omega_\sigma}\rho_\sigma dV = \int_{\Omega_\sigma}\left[\frac{\partial\rho_\sigma}{\partial t} + \nabla\cdot(\rho_\sigma \boldsymbol{u}_\sigma)\right]dV = 0, \tag{9}$$

$$\frac{\partial\rho_\sigma}{\partial t} + \nabla\cdot(\rho_\sigma \boldsymbol{u}_\sigma) = 0, \tag{10}$$

$$\frac{\partial\rho_\sigma}{\partial t} + \nabla\cdot(\rho_\sigma \boldsymbol{u}) = -\nabla\cdot\boldsymbol{j}_\sigma, \tag{11}$$

$$\frac{\partial n_\sigma}{\partial t} + \nabla\cdot(n_\sigma \boldsymbol{v}) = -\nabla\cdot\boldsymbol{k}_\sigma. \tag{12}$$

The last two equations are two equivalent formulations of the species transport equation. However they already allow to point out a fundamental distinction [2], which will clarified later on by discussing the kinetic modeling.

> (!!) Equation (10) assumes as unknown variables of the calculation the single species quantities ρ_σ and $\boldsymbol{u}_\sigma$. Obviously in order to solve this system of equations some additional equations for $\boldsymbol{u}_\sigma$ must be provided. If N is the number of species, this means $N\times(1+D)$ (where D is the number of physical dimensions) equations to be solved. This strategy defines the so-called *multi-fluid* approach.
>
> (!!) Equation (11) or Equation (12) assumes as unknown variables of the calculation the quantities ρ_σ (n_σ) and $\boldsymbol{u}$ ($\boldsymbol{v}$), where the latter is unique for all the species. Obviously in order to solve this system of equations an additional equation for $\boldsymbol{u}$ ($\boldsymbol{v}$) and some phenomenological correlations for $\boldsymbol{j}_\sigma$ ($\boldsymbol{k}_\sigma$) must be provided. The phenomenological correlations for $\boldsymbol{j}_\sigma$ ($\boldsymbol{k}_\sigma$) allow one to compute these terms by means of the main unknowns, i.e. ρ_σ (n_σ) and $\boldsymbol{u}$ ($\boldsymbol{v}$). If N is the number of species, this means $N + D \leq N\times(1+D)$ equations to be solved. This strategy defines the so-called *single-fluid* approach.

[2] In multi-phase modeling, the continuous phase models (CPM) can be usually divided in two sets: those coherent with the single-fluid approach (e.g. Mixture models) and those coherent with the multi-fluid approach (e.g. Eulerian-Eulerian models, Eulerian-granular models).

Obviously the latter approach ensures a reduction of the number of equations to be solved (for $N > 1$), but it forces one to introduce some proper phenomenological correlations: in the following, the Fick model and the Maxwell-Stefan model will be discussed.

2.3 Fick model

A very popular phenomenological model (or law) for expressing the diffusion fluxes based on experimental studies involving binary mixtures is the Fick model [2]. Let us identify by 1 and 2 the two components of the binary mixture (this is for highlighting that some of the properties of this model are not general, but they depend on considering two components only). Hence the Fick model can be expressed as

$$\boldsymbol{k}_1 = -nD_{12}\nabla y_1, \tag{13}$$

where D_{12} is the *binary Fick diffusion* coefficient (it is always better to refer the diffusion coefficients to the original models, because their definitions are not unique), or equivalently

$$\nabla y_1 = -\frac{\boldsymbol{k}_1}{nD_{12}} = -\frac{\boldsymbol{k}_1 - y_1(\boldsymbol{k}_1 + \boldsymbol{k}_2)}{nD_{12}} = -\frac{y_2\boldsymbol{k}_1 - y_1\boldsymbol{k}_2}{nD_{12}} = -\frac{y_1 y_2}{D_{12}}(\boldsymbol{u}_1 - \boldsymbol{u}_2). \tag{14}$$

Let us suppose to adopt the single-fluid approach. Consequently our unknows becomes n_σ and $\boldsymbol{v}$. Let us suppose to consider a binary mixture and to use the Fick model in order to expressed the diffusion fluxes. Finally let us consider the low Mach number limit for the barycentric flow, which implies a barycentric velocity nearly diverge-free ($\nabla \cdot \boldsymbol{u} \approx 0$ and consequently $\nabla \cdot \boldsymbol{v} \approx 0$) and consequently a total density field nearly constant. Finally let us consider a mixture characterized by modest concentration gradients such as the total molecular weight, i.e. $1/m = \sum_\varsigma (x_\varsigma/m_\varsigma)$, is nearly independent of the local mass concentrations. Neglecting the divergence of the total velocity, the gradients of the total mixture density and those of the total molecular weight yields

$$\frac{\partial y_1}{\partial t} + \boldsymbol{v} \cdot \nabla y_1 = D_{12}\nabla^2 y_1, \tag{15}$$

where D_{12} is assumed constant. The previous equation is the result of the so-called linearized theory, which allows one to recover an advection-diffusion equation for the single component concentration[3].

> (!!) Equation (15) is a simplified version of the operative equation considered by the *passive-scalar* approach. Essentially according to this strategy, the dynamics of the single species is described only by tracing the corresponding molar concentration y_σ, due to a given velocity field $\boldsymbol{v}$.

In this lecture, the problem of finding reliable experimental expressions for the transport coefficients will not be discussed. However a lot of experimental data have been already collected [3].

[3] In the following, the Fick model will be generalized in order to include a tensor $\boldsymbol{D}$ of diffusion coefficients. In this case, exploiting the properties of the corresponding modal matrix, it is possible to make diagonal the diffusion tensor $\boldsymbol{D}$ so that the problem reduces to finite a set of uncoupled advection-diffusion equations. This means that the previous discussion is not so particular.

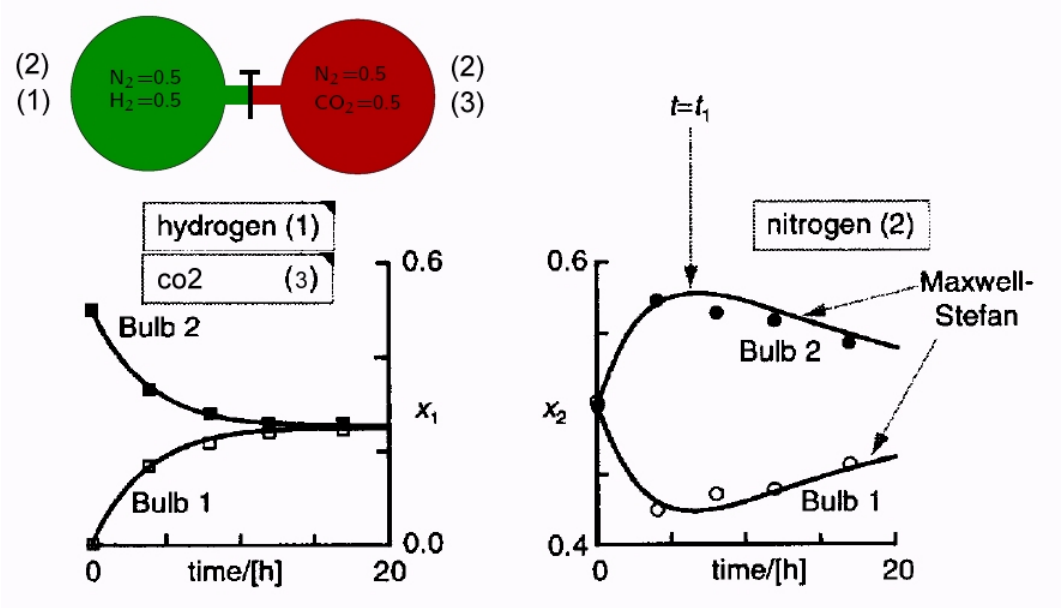

Figure 1: Experimental set-up of the experiment conducted by Duncan & Toor (1962) and main results [4].

2.4 Limits of Fick model: osmotic diffusion, reverse diffusion and diffusion barrier

Even though the Fick model is very simple, it shows some serious drawback when more than two species are considered [4]. In order to realize this, let us consider the following experiment conducted by Duncan & Toor (1962). These authors examined the diffusion in an ideal ternary gas mixture made of hydrogen (1) nitrogen (2) and carbon dioxide (3). The experimental set-up consisted of two bulb diffusion cells, pictured in Fig. 1.

The bulbs, bulb A and bulb B, had the initial compositions given below:

$$\begin{aligned} \text{Bulb A} \quad &: \quad y_1 = 0.00000,\ y_2 = 0.50086,\ y_3 = 0.49914, \\ \text{Bulb B} \quad &: \quad y_1 = 0.50121,\ y_2 = 0.49879,\ y_3 = 0.00000. \end{aligned}$$

At the time $t = 0$, the stopcock separating the two composition environments at the center of the capillary connecting the two bulbs was opened and diffusion of the three species was allowed to take place. The composition-time trajectories for each of the three diffusing species in either bulb has been presented in Fig. 1. Let us first examine what happens to hydrogen (1) and carbon dioxide (3). The composition-time trajectories are as we should expect. The diffusion behavior of these two species hydrogen and carbon dioxide may be termed to be Fickian, i.e. down their respective composition gradients.

However if we examine the composition-time trajectory of nitrogen (2), we see several curious phenomena. Initially, the compositions of nitrogen in the two bulbs are almost identical and therefore at this point the composition gradient driving force for nitrogen must vanish. However, it was observed experimentally that the diffusion of nitrogen does take

place and this is contrary to the Fickian expectations, since $y_A(t=0) = y_B(t=0)$. In particular, the bulb A composition decreases and continues at the expense of bulb B: this means that this diffusion of nitrogen is in an up-hill direction. Up-hill diffusion of nitrogen continued to take place until a critical time is reached when the composition profiles in wither bulb tend to a plateau. This plateau implies that the diffusion flux of nitrogen is zero at this point despite the fact that there is a large driving force existing. Beyond the critical time, the behavior of nitrogen is again in good agreement with the Fickian predictions.

The previous discussed phenomena are:

- *osmotic diffusion*, namely diffusion of a component despite the absence of a driving force;
- *reverse diffusion*, namely diffusion of a component in a direction opposite to that dictated by its driving force;
- *diffusion barrier*, namely diffusion flux is zero despite a large driving force.

(!!) Clearly this example shows the intrinsic limits of the Fick model. The key problem is that in the Fick model each molar flux is driven only by the corresponding molar concentration gradient. Each species behaves on its own. In particular this problem can be corrected by taking into account the mutual interactions among the species.

2.5 Maxwell-Stefan model

In case of more than two species, Equation (14) can be generalized by the Maxwell-Stefan model [2, 4], namely

$$\nabla y_\sigma = \sum_\varsigma B_{\sigma\varsigma} y_\sigma y_\varsigma (\boldsymbol{u}_\varsigma - \boldsymbol{u}_\sigma) = \frac{1}{n} \sum_\varsigma B_{\sigma\varsigma} (y_\sigma \boldsymbol{k}_\varsigma - y_\varsigma \boldsymbol{k}_\sigma), \tag{16}$$

where $B_{\sigma\varsigma} = B(m_\sigma, m_\varsigma)$ is the *binary Maxwell-Stefan diffusion resistance* coefficient. An important comment is that the previous parameter only depends (according to the results of the kinetic theory) on the molecular weights of considered species and on the total pressure and temperature (thermodynamic variables identifying the mixture equilibrium state). A graphical representation of this model is reported in Fig. 2.

It is possible to directly compare the previous expression with the Fick expression in some simple limiting cases. Let us consider a ternary mixture, like that discussed in the Duncan & Toor experiment, namely

$$-n\nabla y_1 = (B_{12} y_2 + B_{13} y_3)\boldsymbol{k}_1 - B_{12} y_1 \boldsymbol{k}_2 - B_{13} y_1 \boldsymbol{k}_3. \tag{17}$$

In case of a solvent species, i.e. $y_1 \to 0$, $y_2 \to 0$ and then consequently $y_3 \to 1$, the previous expression becomes $-n\nabla y_1 = B_{13}\boldsymbol{k}_1$ and hence the consistency with the Fick model is recovered by selecting $1/D_{12} = B_{13}$. Another example is the case of a dilute species, i.e. $y_1 \to 0$, in this case the consistency requires $1/D_{12} = B_{12} y_2 + B_{13} y_3$.

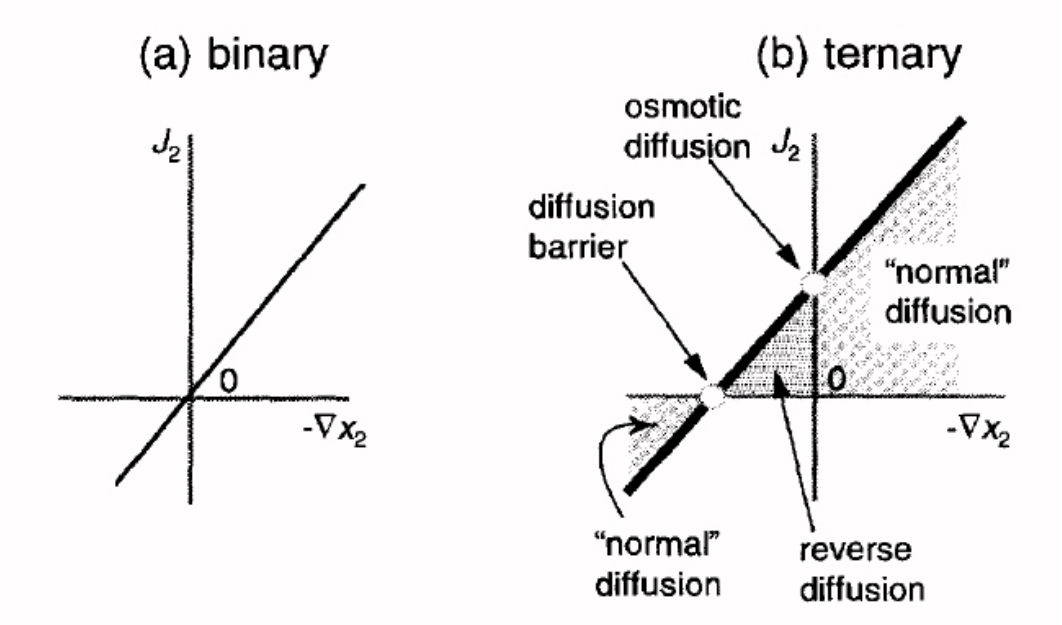

Figure 2: Graphical representation of the Maxwell-Stefan model for ternary system [4].

The previous examples prove that, in some limiting cases, it is possible to recover the results of the Maxwell-Stefan model by means of a simpler model and by selecting properly the values of the diffusion coefficient. In general it is possible to express the previous expression for the Maxwell-Stefan model by means of a tensorial notation, namely $-n[\nabla y] = [\boldsymbol{R}][\boldsymbol{k}]$, where $[\boldsymbol{k}]$ collects in a single vector the components of all the single-species diffusion vectors, $[\nabla y]$ collects all the components of the single-species concentration gradients and $[\boldsymbol{R}] = [\boldsymbol{R}(m_\sigma, y_\sigma)]$ is a tensor with proper size. The generalization of the Fick model is possible by $[\boldsymbol{k}] = -n[\boldsymbol{D}][\nabla y]$ where $[\boldsymbol{D}(m_\sigma, y_\sigma)] = [\boldsymbol{R}]^{-1}$.

> (!!) The last argumentation is not completely convincing. In fact, $[\boldsymbol{R}(m_\sigma, y_\sigma)]$ is a tensor which depends on the local concentrations (unlike the tensor $B_{\sigma\varsigma}$). This means that in some points the inverse of the tensor $[\boldsymbol{R}]$ may not be defined. This is a serious problem if the passive scalar approach is adopted because, in this case, the diffusion fluxes must be expressed since they are not original unknowns.

3 Kinetic modeling

3.1 Boltzmann equations

We will discuss succinctly the kinetic theory for mixtures. The simultaneous Boltzmann equations for a mixture without external force can be written as:

$$\partial_t f_\sigma + \boldsymbol{\xi} \cdot \boldsymbol{\nabla} f_\sigma = Q_\sigma, \tag{18}$$

where $Q_\sigma = \sum_\varsigma Q_{\sigma\varsigma}$ and $Q_{\sigma\varsigma} = Q_{\varsigma\sigma}$, $\varsigma \neq \sigma$, is the cross collision term for two different species σ and ς. Obviously, for an N-component system, there will be N such equations. In general, the collision term is

$$Q_{\sigma\varsigma} = \int d\boldsymbol{\xi}_\varsigma d\Theta d\varepsilon B(\Theta, \|\boldsymbol{\xi}_{\sigma\varsigma}\|)[f'_\sigma f'_\varsigma - f_\sigma f_\varsigma], \tag{19}$$

where f'_σ (f'_ς) and f_σ (f_ς) denote the post-collision and pre-collision state of the particle of species σ (ς), respectively, $\boldsymbol{\xi}_{\sigma\varsigma} = \boldsymbol{\xi} - \boldsymbol{\xi}_\varsigma$, and we refer the details of the collision integral of Eq. (19) to standard texts on the Boltzmann equation [3, 5, 6, 7, 8].

Obviously, the system of N equations for N species is much more formidable to analyze than the Boltzmann equation for a single-species system. Before proceeding with simplified expressions, it is worth the effort to compute the following integral [9]

$$\int \boldsymbol{\xi} Q_\sigma d\boldsymbol{\xi} = p \sum_\varsigma B_{\sigma\varsigma} y_\sigma y_\varsigma (\boldsymbol{u}_\varsigma - \boldsymbol{u}_\sigma), \tag{20}$$

where now the Maxwell-Stefan diffusion resistance coefficient $B_{\sigma\varsigma}$ can be interpreted as macroscopic consequence of the interaction potential between species σ and ς.

> (!!) The previous expression is of fundamental importance, because it naturally shows the link between the kinetic description and the phenomenological coefficients involved in Maxwell-Stefan model. Actually the latter can be computed as functions of the interaction potentials only. Moreover the exchange of momentum among the species prescribed by the Maxwell-Stefan model is firmly based on the continuous Boltzmann equations.

In modeling of an N-species system, the first objective is to find a suitable approximation for the integral collision term of Eq. (19) that would significantly simplify the computation while maintaining the most essential part of the physics. For this purpose, the linearized or relaxation collision models are applied [7, 8, 10].

The justification for the relaxation approximation for the collision terms relies on our understanding of the underlying physics pertinent to mixtures. In a system of multiple species, there are a number of competing equilibration processes occurring simultaneously. The approach to equilibrium in the system can be roughly divided into two stages.

- In the first stage, each individual species equilibrates within itself so that its local distribution function relaxes to a *local* Maxwellian, and this process of individual equilibration is referred to as Maxwellization.

- In the second stage, the entire system equilibrates so that the velocity and temperature differences among different species vanish eventually.

Obviously the equilibrating process of a multi-species system involves a number of different time scales. In addition, the Maxwellization itself can take place in various scenarios depending on the molecular weights and mass fractions of the interacting species.

Consider two binary mixtures, for example, each consisting of a light and a heavy gas. The total mass of each species is equal for one mixture, implying a smaller number density for

the heavier gas, and the number densities of the two species is equal for the other, implying a larger mass density (or mass fraction) for the heavier species. In equal-mass mixture, the Maxwellization of light species is mostly due to self-collision whereas the equilibration of the heavier species is predominantly due to *cross collisions*. This is due to the fact that the number of heavy molecules available for collisions is smaller. In the equal-number mixture, Maxwellization of both species involves *self and cross collisions*. This example illustrates the equilibrating process in a mixture depends strongly on the properties of the mixture. When the Maxwellization process is complete, the stress of the corresponding species becomes isotropic, or equivalently the heat conduction relaxes to zero. Therefore, the scale on which the stress becomes isotropic or the heat conduction relaxes is a suitable measure of Maxwellization. The equilibration among different species can also take place in several different manners. Velocity and temperature differences may equilibrate on the same temporal scale, as in the equal-mass mixture, or on vastly different scales, as in the equal-number mixture. In addition, these equilibrating processes need not to occur sequentially but also concurrently with the Maxwellization [11].

There is a significant amount of literature on gas mixtures within the framework of kinetic theory [5, 10, 12, 13, 14, 15, 16, 17, 18, 19, 20, 21, 22]. In the Chapman-Enskog analysis for a simple gas, one assumes a clear separation of scales in space and time, that is, to distinguish the spatial and temporal scales which are much larger than the mean free path or mean free time, respectively. An analogy for a mixture becomes much more difficult because of multiplicity of spatial and temporal scales due to inter-species interactions. In the work of Chapman and Cowling [5], the full Boltzmann equations for a binary mixture are analyzed under the assumptions that all scales are of the same order approximately, or equivalently, that the phenomenon of interest is smooth with respect to all collisional scales. The determination of various transport coefficients was the main objective of Chapman and Cowling [5] and no attempt was made to describe the evolution dynamics for mixtures [11].

3.2 Traditional BGK models

For realistic systems of engineering interest, direct analysis or numerical simulation of the Boltzmann equation is not feasible in general. This is due to the difficulty involved in evaluating the complex integral collision operators. Two approaches can be followed to circumvent this difficulty. The first, Grad's moment method, is to obtain the non-normal solutions of the Boltzmann equation (*i.e.*, the solutions beyond the hydrodynamic variables) [23]. The Boltzmann equation is equivalent to system of infinite number of moment equations. In the Grad's moment method, the moment system is truncated to a finite number of moments and closure modeling is required to express the unclosed moments in terms of the closed ones. And the second is to derive simplified model Boltzmann equations which are more manageable to solve. Numerous model equations are influenced by Maxwell's approach to solve the Boltzmann equation by using the properties of the Maxwell molecule [24] and the linearized Boltzmann equation. The simplest model equations for a binary mixture is that by Gross and Krook [13], which is an extension of the single-relaxation-time model for a pure system — the celebrated Bhatnagar-Gross-Krook (BGK) model [25].

With the BGK approximation [25, 13], the collision integrals $Q_{\sigma\varsigma}$ [σ, $\varsigma \in$ (A, B)] can be

approximated by following linearized collision terms

$$J_{\sigma\sigma} = -\frac{1}{\tau_\sigma}[f_\sigma - f_{\sigma(0)}], \qquad J_{\sigma\varsigma} = -\frac{1}{\tau_{\sigma\varsigma}}[f_\sigma - f_{\sigma\varsigma(0)}], \tag{21}$$

where $f_{\sigma(0)}$ and $f_{\sigma\varsigma(0)}$ are Maxwellians

$$f_{\sigma(0)}(\rho_\sigma, \boldsymbol{u}_\sigma, T_\sigma) = \frac{\rho_\sigma}{(2\pi R_\sigma T_\sigma)^{D/2}} e^{-(\boldsymbol{\xi}-\boldsymbol{u}_\sigma)^2/(2R_\sigma T_\sigma)}, \tag{22a}$$

$$f_{\sigma\varsigma(0)}(\rho_\sigma, \boldsymbol{u}_{\sigma\varsigma}, T_{\sigma\varsigma}) = \frac{\rho_\sigma}{(2\pi R_\sigma T_{\sigma\varsigma})^{D/2}} e^{-(\boldsymbol{\xi}-\boldsymbol{u}_{\sigma\varsigma})^2/(2R_\sigma T_{\sigma\varsigma})}, \tag{22b}$$

where D is the spatial dimension, $R_\sigma = k_B/m_\sigma$ and m_σ are the gas constant and the molecular mass of the σ species, respectively, and k_B is the Boltzmann constant. There are three adjustable relaxation parameters in the collision terms: τ_σ, τ_ς, and $\tau_{\sigma\varsigma} = (\rho_\varsigma/\rho_\sigma)\tau_{\varsigma\sigma}$. The species Maxwellian $f_{\sigma(0)}$ is characterized by the conserved variables of each individual species: the mass density ρ_σ, the mass velocity $\boldsymbol{u}_\sigma$, and the temperature T_σ; while the mixture Maxwellians $f_{\sigma\varsigma(0)}$ and $f_{\varsigma\sigma(0)}$ are characterized by four adjustable parameters: $\boldsymbol{u}_{\sigma\varsigma}$, $\boldsymbol{u}_{\varsigma\sigma}$, $T_{\sigma\varsigma}$, and $T_{\varsigma\sigma}$. There are several considerations in determining these arbitrary parameters: simplicity of the resulting theory, accuracy of approximation, and ease of computation. The cross-collisional terms would be symmetric only if one takes $\boldsymbol{u}_{\sigma\varsigma} = \boldsymbol{u}_{\varsigma\sigma} = \boldsymbol{u}$ and $T_{\sigma\varsigma} = T_{\varsigma\sigma} = T$, where $\boldsymbol{u}$ and T are the velocity and temperature of the mixture, which are yet to be defined. This is essential in preserving the irreversible thermodynamics, especially the Onsager relation [26]. Another thermodynamic relation needs to be satisfied is the Indifferentiability Principle [9], that is, if two species are identical, the system of the mixture equations (18) collapses the equation of a pure species. Obviously, this is true for the Boltzmann equation, but it does not hold for the BGK-type model equations for mixtures. As we shall see later, the constraints imposed by the Indifferentiability Principle would also affect the self collision terms.

Since a mixture ultimately relaxes to the equilibrium defined by the mixture variables $\boldsymbol{u}$ ant T, it is logical to use $f_{\sigma\varsigma(0)}$ as the equilibrium in the Chapman-Enskog analysis. Fewer terms in the expansion of f_σ about $f_{\sigma\varsigma(0)}$ would be needed in many cases if one chooses $\boldsymbol{u}_{\sigma\varsigma} = \boldsymbol{u}_\sigma$ and $T_{\sigma\varsigma} = T_\sigma$, *i.e.*, $f_{\sigma\varsigma(0)} = f_{\sigma(0)}$. The main difference in using the mixture variables $\boldsymbol{u}$ and T, as opposed to the species variables $\boldsymbol{u}_\sigma$ and T_σ is that the former leads to the single-fluid theory, from which one set of hydrodynamic equations for the mixture variables is derived, while the latter leads to the multi-fluid theory [15, 21], from which two sets of coupled hydrodynamic equations of mixture variables can be derived.

> (!!) However the distinction between single-fluid and multi-fluid approach mainly depends on how many equations at kinetic level are solved and how the numerical results are collected at macroscopic level in order to produce the mixture description.

For σ species, the BGK-type collision term combining self- and cross-collisions can be rewritten as:

$$J_\sigma = -\left(\frac{1}{\tau_\sigma} + \frac{1}{\tau_{\sigma\varsigma}}\right)[f_\sigma - f_{\sigma(0)}] - \frac{1}{\tau_{\sigma\varsigma}}[f_{\sigma(0)} - f_{\sigma\varsigma(0)}]. \tag{23}$$

Mathematically, $f_{\sigma(0)}$ can be expanded in terms of $f_{\sigma\varsigma(0)}$, equivalently, the fluid properties of individual species, ρ_σ, $\boldsymbol{u}_\sigma$, and T_σ in terms of the mixture fluid properties, ρ, $\boldsymbol{u}$, and T, or *vice versa*. As pointed out by Gross and Krook [13], and similarly by Hamel [17, 19], one can also linearly combine these two expansions with an adjustable parameter $0 \le \beta \le 1$, that is, a portion of $f_{\sigma(0)}$, $\beta f_{\sigma(0)}$, is expressed in terms of $f_{\sigma\varsigma(0)}$, and a portion of $f_{\sigma\varsigma(0)}$, $(1-\beta)f_{\sigma\varsigma(0)}$, is expressed in terms $f_{\sigma(0)}$:

$$\begin{aligned} & f_{\sigma(0)} - f_{\sigma\varsigma(0)} = n_\sigma (2\pi R_\sigma T)^{-3/2} \left(e^{-c_\sigma^2/2R_\sigma T} - e^{-c^2/2R_\sigma T} \right) \\ = \;& (1-\beta) f_{\sigma(0)} \left[1 - e^{-(2\boldsymbol{c}_\sigma + \boldsymbol{w}_\sigma)\cdot \boldsymbol{w}_\sigma / 2R_\sigma T} \right] - \beta f_{\sigma\varsigma(0)} \left[1 - e^{(2\boldsymbol{c} - \boldsymbol{w}_\sigma)\cdot \boldsymbol{w}_\sigma / 2R_\sigma T} \right], \end{aligned} \tag{24}$$

where $\boldsymbol{c} = \boldsymbol{\xi} - \boldsymbol{u}$, $\boldsymbol{c}_\sigma = \boldsymbol{\xi} - \boldsymbol{u}_\sigma$, $\boldsymbol{w}_\sigma = \boldsymbol{u}_\sigma - \boldsymbol{u}$, and we have assumed the mixture is isothermal, *i.e.*, $T_\sigma = T_{\sigma\varsigma} = T$.

If the cross-collision term is linearized in terms of the diffusion velocity $\boldsymbol{w}_\sigma$, one obtains the generalized model of Sirovich [15, 27]:

$$J_\sigma = -\frac{1}{\tau_\sigma}[f_\sigma - f_{\sigma(0)}] - \frac{1}{\tau_{\sigma\varsigma}} \boldsymbol{s}_\sigma \cdot \boldsymbol{w}_\sigma, \tag{25}$$

where

$$\boldsymbol{s}_\sigma = \frac{1}{R_\sigma T} \left[(1-\beta) f_{\sigma(0)} (\boldsymbol{\xi} - \boldsymbol{u}_\sigma) + \beta f_{\sigma\varsigma(0)} (\boldsymbol{\xi} - \boldsymbol{u}) \right]. \tag{26}$$

The original model of Sirovich [15] is recovered when $\beta = 0$. This model allows two relaxation times, consequently a variable Schmidt number Sc independent of the Reynolds number Re.

So far we have yet to define the mixture velocity $\boldsymbol{u}$ and temperature T. The choice of $\boldsymbol{u}$ and T is *unique* and is a key issue in the BGK-type of modeling. By insisting that the relaxation equations for the velocity difference $(\boldsymbol{u}_\sigma - \boldsymbol{u}_\varsigma)$ and the temperature difference $(T_\sigma - T_\varsigma)$ obtained from the full Boltzmann equations and the model equations must be the same, the following definitions for the mixture velocity and temperature must be used [16]:

$$\boldsymbol{u} = \boldsymbol{u}_{\sigma\varsigma} = \boldsymbol{u}_{\varsigma\sigma} = \frac{m_\sigma \boldsymbol{u}_\sigma + m_\varsigma \boldsymbol{u}_\varsigma}{m_\sigma + m_\varsigma}, \tag{27a}$$

$$T_{\sigma\varsigma} = T_\sigma + \frac{2 m_\sigma m_\varsigma}{(m_\sigma + m_\varsigma)^2} \left[(T_\varsigma - T_\sigma) + \frac{m_\varsigma}{6k_B} (\boldsymbol{u}_\varsigma - \boldsymbol{u}_\sigma)^2 \right]. \tag{27b}$$

However, the above definition of $\boldsymbol{u}$ for the BGK model equations contradicts the Indifferentiability Principle [9]. That is, for two identical species σ and ς, the model equations do not reduce to the one for a single species gas. For the BGK model equations of mixtures, the Indifferentiability Principle can be maintained if the barycentric velocity is used in the mixture Maxwellian:

$$\boldsymbol{u} = \frac{\rho_\sigma \boldsymbol{u}_\sigma + \rho_\varsigma \boldsymbol{u}_\varsigma}{\rho_\sigma + \rho_\varsigma}. \tag{28}$$

But the barycentric velocity is inconsistent with the conditions (27a) derived from the full Boltzmann equations. Hence a dilemma arises: between the consistency with the full Boltzmann equations and the Indifferentiability Principle, which one to maintain? As we will argue next, the Indifferentiability Principle is more important for the hydrodynamic modeling of mixtures considered here.

(!!) It is simple to realize the importance of the Indifferentiability Principle. If for identical particles, the model equations do not reduce to one for a single species gas, this means that some inconsistencies may exist, *even in the macroscopic transport equations*.

3.3 Advanced BGK models

In order to discriminate the possible simplified models, some consistency constraints must be considered first. The basic consistency constraints [9] in the design of simplified kinetic models for mixture modeling are the following.

1. The simplified model should satisfy the Indifferentiability Principle [28], which prescribes that, if a BGK-like equation for each species is assumed, this set of equations should reduce to a single BGK-like equation, when mechanically identical components are considered (*microscopic formulation*). This essentially means that, when all the species are identical, one should recover at macroscopic levels the equations governing the single component gas dynamics (*macroscopic formulation*). This property is satisfied by the bilinearity of the collision operators in the full Boltzmann equations for mixtures.

2. The relaxation equations for momentum and temperature, i.e. the equations describing the time decay of the momentum and temperature differences among the species, should be as close as possible to those derived by means of the full Boltzmann equations.

3. All the species should tend to a target equilibrium distribution which is a Maxwellian, centered on a proper macroscopic velocity, common to all the species.

4. The non-negativity of the distribution functions for all the species should be satisfied.

5. A generalized H theorem for mixtures should hold.

Unfortunately it is well known that, in the framework of the Lattice Boltzmann Method (LBM), both issue (4) concerning the non-negativity of the distribution functions [29], which is valid only asymptotically in the limit of low Mach number, and issue (5) concerning the existence of an H theorem, cannot be satisfied [30]. For these reasons, the following discussion will focus on the first three issues only.

(!!) In the following, for sake of simplicity, only the isothermal models will be considered, i.e. $T_\sigma = T$ for any σ, since the main interested is focused on isothermal diffusion.

The key idea is to discuss the advanced BGK model proposed by Andries et al.[9] in case of isothermal flow, in order to simplify it and to highlight the main features. This model is based on only one *global* (i.e., taking into account all the species ς) operator for each species σ, namely

$$\partial_t f_\sigma + \boldsymbol{\xi}\cdot\boldsymbol{\nabla} f_\sigma = \lambda_\sigma \left[f_{\sigma(*)} - f_\sigma \right], \tag{29}$$

where $\lambda_\sigma = 1/\tau_\sigma$ is the relaxation time frequency and the local equilibrium is defined by

$$f_{\sigma(*)} = \frac{\rho_\sigma}{(2\pi e_\sigma)^{D/2}} \exp\left[-\frac{(\boldsymbol{\xi} - \boldsymbol{u}_*)^2}{2\, e_\sigma}\right], \tag{30}$$

where $e_\sigma = R_\sigma T$ is the internal energy for species σ and finally $\boldsymbol{u}^*_\sigma$ is a proper (undefined) macroscopic velocity representative of the whole mixture.

In order to derive the expression for the undefined velocity, we recall Eq. (20) and we define $\boldsymbol{u}^*_\sigma$ such as that the latter condition is satisfied as well for the simplified BGK model, i.e. that the BGK model ensures the same exchange of momentum among the species, namely

$$\lambda_\sigma \rho_\sigma \left(\boldsymbol{u}^*_\sigma - \boldsymbol{u}_\sigma\right) = p \sum_\varsigma B_{\sigma\varsigma} y_\sigma y_\varsigma (\boldsymbol{u}_\varsigma - \boldsymbol{u}_\sigma), \tag{31}$$

or equivalently

$$\boldsymbol{u}^*_\sigma = \boldsymbol{u}_\sigma + \frac{p}{\lambda_\sigma \rho_\sigma} \sum_\varsigma B_{\sigma\varsigma} y_\sigma y_\varsigma (\boldsymbol{u}_\varsigma - \boldsymbol{u}_\sigma). \tag{32}$$

Actually the relaxation frequency λ_σ is undefined and its choice is crucial for the complete model [9]. Fortunately in our simplified case, it is much easier to select these parameters. In particular, let us consider the limiting case of all identical species, i.e. $m_\sigma = m$, which is the same limiting case considered by the Indifferentiability Principle. In this case, the previous expression reduces to

$$\boldsymbol{u}^*_\sigma = \boldsymbol{u}_\sigma + \frac{p\, B_{m\,m}}{\lambda_\sigma \rho} (\boldsymbol{u} - \boldsymbol{u}_\sigma). \tag{33}$$

If and only if $\lambda_\sigma = \lambda = p\, B_{m\,m}/\rho$, then $\boldsymbol{u}^*_\sigma = \boldsymbol{u}$ (barycentric velocity) and summing Eqs. (29) over the species yields

$$\partial_t f + \boldsymbol{\xi} \cdot \boldsymbol{\nabla} f = \lambda \left[f_{(m)} - f\right], \tag{34}$$

where $f = \sum_\sigma f_\sigma$ and $f_{(m)}$ is defined by

$$f_{(m)} = \frac{\rho}{(2\pi e)^{D/2}} \exp\left[-\frac{(\boldsymbol{\xi} - \boldsymbol{u})^2}{2\, e}\right], \tag{35}$$

where $e_\sigma = RT$, $R = R_0/m$ and R_0 is the universal gas constant. Clearly this model satisfies the Indifferentiability Principle. The derived condition does allow one to define uniquely the relaxation frequency in a generic case, i.e. $\lambda_\sigma = p\, B_{\sigma\sigma}/\rho$. Substituting in the previous expression yields

$$\boldsymbol{u}^*_\sigma = \boldsymbol{u}_\sigma + \sum_\varsigma \frac{m^2}{m_\sigma m_\varsigma} \frac{B_{\sigma\varsigma}}{B_{\sigma\sigma}} x_\varsigma (\boldsymbol{u}_\varsigma - \boldsymbol{u}_\sigma). \tag{36}$$

(!!) The previous expression completely defines the macroscopic velocity considered by the model for the definition of the local equilibrium. This velocity is a bit different from those usually used in order to characterize the mixture dynamics.

Let us consider the following additional property. Multiplying Eq. (36) by ρ_σ and summing over all the species yields

$$\sum_\sigma \rho_\sigma \boldsymbol{u}_\sigma^* = \rho \boldsymbol{u} + \rho \sum_\sigma \sum_\varsigma \frac{m^2}{m_\sigma m_\varsigma} \frac{B_{\sigma\varsigma}}{B_{\sigma\sigma}} x_\sigma x_\varsigma (\boldsymbol{u}_\varsigma - \boldsymbol{u}_\sigma) = \rho \boldsymbol{u}, \tag{37}$$

or equivalently $\sum_\varsigma x_\varsigma \boldsymbol{u}_\varsigma^* = \boldsymbol{u} = \sum_\varsigma x_\varsigma \boldsymbol{u}_\varsigma$.

4 Lattice Boltzmann scheme

4.1 Basic BGK equation

In order to derive the simplest lattice Boltzmann scheme for the previous model, let us recall first the model equation, where the Boltzmann scaling is highlighted by using the quantities with hat, namely

$$\frac{\partial \hat{f}_\sigma}{\partial \hat{t}} + \xi_i \frac{\partial \hat{f}_\sigma}{\partial \hat{x}_i} = \lambda_\sigma \left[\hat{f}_{\sigma(*)} - \hat{f}_\sigma \right], \tag{38}$$

where $\hat{x}_i$, $\hat{t}$, and ξ_i are the (dimensionless) space coordinates, time, and molecular velocity components, respectively; $\hat{f}_\sigma(\hat{t}, \hat{x}_i, \xi_i)$; λ_σ is a positive constant of the order of unit; and finally $\hat{f}_{\sigma(*)}(\hat{t}, \hat{x}_i, \xi_i)$ is the equilibrium distribution function for the species σ, namely

$$\hat{f}_{\sigma(*)} = \frac{\rho_\sigma}{2\,\pi\varphi_\sigma/3} \exp\left[-\frac{3\,(\xi_i - u_{\sigma i}^*)^2}{2\,\varphi_\sigma} \right], \tag{39}$$

where $u_{\sigma i}^*$ is defined by Eq. (36),

$$\rho_\sigma = \ll \hat{f}_\sigma \gg, \qquad q_{\sigma i} = \rho_\sigma u_{\sigma i} = \ll \xi_i \hat{f}_\sigma \gg, \tag{40}$$

and

$$\ll \cdot \gg = \int_{-\infty}^{+\infty} (\cdot)\, d\xi_1 d\xi_2. \tag{41}$$

> (!!) The parameter φ_σ is introduced in order to take into account of different molecular weights m_σ and consequently different internal energies e_σ for the species.

Recall that the unit of space coordinate and that of time variable in Eq. (38) are the mean free path $l_c (= cT_c)$ and the mean collision time T_c, respectively. Obviously, they are not appropriate as the characteristic scales for flow field in the continuum limit. Let the characteristic length scale of the flow field be L and let the characteristic flow speed be U. There are two factors in the limit we are interested in. The continuum limit means $l_c \ll L$ and the low speed limit means $U \ll c$. In the following asymptotic analysis, we introduce the other dimensionless variables, defined by

$$x_i = (l_c/L)\hat{x}_i, \qquad t = (UT_c/L)\hat{t}. \tag{42}$$

Defining the small parameter ϵ as $\epsilon = l_c/L$, which corresponds to the Knudsen number, we have $x_i = \epsilon \hat{x}_i$. Furthermore, assuming

$$U/c = \epsilon, \tag{43}$$

which is the key of derivation of the low Mach number limit [31], we have $t = \epsilon^2 \hat{t}$. Then, Eq. (38) is rewritten as

$$\epsilon^2 \frac{\partial f_\sigma}{\partial t} + \epsilon \xi_i \frac{\partial f_\sigma}{\partial x_i} = \lambda_\sigma \left[f_{\sigma(*)} - f_\sigma \right], \tag{44}$$

where $f_\sigma(t, x_i, \xi_i)$ and $f_{\sigma(*)}(t, x_i, \xi_i)$. In this new scaling, we can assume

$$\frac{\partial f}{\partial \alpha} = O(f), \qquad \frac{\partial M}{\partial \alpha} = O(M), \tag{45}$$

where $f = f_{\sigma(*)}, f_\sigma$ and $\alpha = t, x_i$ and $M = \rho_\sigma, q_{\sigma i}$.

Since LBM does not need to give the accurate behavior of rarefied gas flows, a simplified kinetic equation, such as the discrete velocity model of isothermal BGK equation with constant collision frequency is often employed as its theoretical basis, namely

$$\epsilon^2 \frac{\partial f_\sigma}{\partial t} + \epsilon V_i \frac{\partial f_\sigma}{\partial x_i} = \lambda_\sigma \left[f_{\sigma(*)} - f_\sigma \right], \tag{46}$$

where V_i is a list of i-th components of the velocities in the considered lattice and $f = f_{\sigma(*)}, f_\sigma$ is a list of discrete distribution functions corresponding to the velocities in the considered lattice.

> (!!) Change in notation: now $f = f_{\sigma(*)}, f_\sigma$ is a list of discrete distribution functions corresponding to the velocities in the considered lattice.

Let us consider the two dimensional 9 velocity model, which is called D2Q9. In D2Q9 model, the molecular velocity V_i has the following 9 values:

$$V_1 = \left[\begin{array}{ccccccccc} 0 & 1 & 0 & -1 & 0 & 1 & -1 & -1 & 1 \end{array} \right]^T, \tag{47}$$

$$V_2 = \left[\begin{array}{ccccccccc} 0 & 0 & 1 & 0 & -1 & 1 & 1 & -1 & -1 \end{array} \right]^T. \tag{48}$$

The components of the molecular velocity V_1 and V_2 are the lists with 9 elements. Before proceeding to the definition of the local equilibrium function $f_{\sigma(*)}$, we define the rule of computation for the list. Let h and g be the lists defined by $h = [h_0, h_1, h_2, \cdots, h_8]^T$ and $g = [g_0, g_1, g_2, \cdots, g_8]^T$. Then, hg is the list defined by $[h_0 g_0, h_1 g_1, h_2 g_2, \cdots, h_8 g_8]^T$. The sum of all the elements of the list h is denoted by $< h >$, i.e. $< h >= \sum_{i=0}^{8} h_i$. Then, the (dimensionless) density ρ_σ and momentum $q_{\sigma i} = \rho_\sigma u_{\sigma i}$ are defined by

$$\rho_\sigma =< f_\sigma >, \qquad q_{\sigma i} =< V_i f_\sigma > . \tag{49}$$

Then, $f_{\sigma(*)}$ is defined by

$$
\begin{aligned}
f_{\sigma(*)} \;=\; & \rho_\sigma \left[1 - 5/9\,\varphi_\sigma - 2/3\,(u^*_{\sigma 1})^2 - 2/3\,(u^*_{\sigma 2})^2,\right. \\
& 1/9\,\varphi_\sigma + 1/3\,(u^*_{\sigma 1}) + 1/3\,(u^*_{\sigma 1})^2 - 1/6\,(u^*_{\sigma 2})^2, \\
& 1/9\,\varphi_\sigma + 1/3\,(u^*_{\sigma 2}) + 1/3\,(u^*_{\sigma 2})^2 - 1/6\,(u^*_{\sigma 1})^2, \\
& 1/9\,\varphi_\sigma - 1/3\,(u^*_{\sigma 1}) + 1/3\,(u^*_{\sigma 1})^2 - 1/6\,(u^*_{\sigma 2})^2, \\
& 1/9\,\varphi_\sigma - 1/3\,(u^*_{\sigma 2}) + 1/3\,(u^*_{\sigma 2})^2 - 1/6\,(u^*_{\sigma 1})^2, \\
& 1/36\,\varphi_\sigma + 1/12\,(u^*_{\sigma 1} + u^*_{\sigma 2}) + 1/8\,(u^*_{\sigma 1} + u^*_{\sigma 2})^2 - 1/24\,(u^*_{\sigma 1})^2 - 1/24\,(u^*_{\sigma 2})^2, \\
& 1/36\,\varphi_\sigma - 1/12\,(u^*_{\sigma 1} - u^*_{\sigma 2}) + 1/8\,(-u^*_{\sigma 1} + u^*_{\sigma 2})^2 - 1/24\,(u^*_{\sigma 1})^2 - 1/24\,(u^*_{\sigma 2})^2, \\
& 1/36\,\varphi_\sigma - 1/12\,(u^*_{\sigma 1} + u^*_{\sigma 2}) + 1/8\,(-u^*_{\sigma 1} - u^*_{\sigma 2})^2 - 1/24\,(u^*_{\sigma 1})^2 - 1/24\,(u^*_{\sigma 2})^2, \\
& \left. 1/36\,\varphi_\sigma + 1/12\,(u^*_{\sigma 1} - u^*_{\sigma 2}) + 1/8\,(u^*_{\sigma 1} - u^*_{\sigma 2})^2 - 1/24\,(u^*_{\sigma 1})^2 - 1/24\,(u^*_{\sigma 2})^2\right]^T .
\end{aligned}
\tag{50}
$$

Clearly ρ_σ can also be obtained as the moment of $f_{\sigma(*)}$, but this not the case for $q_{\sigma i}$:

$$
\rho_\sigma =< f_{\sigma(*)} >, \qquad q^*_{\sigma i} =< V_i f_{\sigma(*)} > \neq q_{\sigma i}. \tag{51}
$$

The coordinates of spatial discrete points (lattice) employed in the LBM computation are $(\hat{x}_1, \hat{x}_2) = (l, m)$, where l and m are integers. Let x^*_i be the coordinate of a lattice point. Then, $x^*_i - V^{(k)}_i$ is the coordinate of a lattice adjacent to the lattice point x^*_i. LBM computation is nothing more than the forward Euler time integration formula of Eq. (46) with the time step of the unity:

$$
f_\sigma(t + \epsilon^2, x_i, V_i) = f_\sigma(t, x_i - V_i\epsilon, V_i) + \lambda_\sigma\, g_\sigma(t, x_i - V_i\epsilon, V_i), \tag{52}
$$

where

$$
g_\sigma = f_{\sigma(*)} - f_\sigma. \tag{53}
$$

The relation to the macroscopic equations will be explained in the next section.

4.2 Asymptotic analysis

The solution of Eq. (52) for small ϵ is investigated in the form of the asymptotic expansion

$$
f_\sigma = f^{(0)}_\sigma + \epsilon f^{(1)}_\sigma + \epsilon^2 f^{(2)}_\sigma + \cdots . \tag{54}
$$

The hydrodynamic moments ρ_σ and $q_{\sigma i}$ are also expanded:

$$
\rho_\sigma = \rho^{(0)}_\sigma + \epsilon \rho^{(1)}_\sigma + \epsilon^2 \rho^{(2)}_\sigma + \cdots , \tag{55}
$$

$$
q_{\sigma i} = \epsilon q^{(1)}_{\sigma i} + \epsilon^2 q^{(2)}_{\sigma i} + \cdots . \tag{56}
$$

Since the Mach number is $O(\epsilon)$, the perturbations of $q_{\sigma i}$ start from the order of ϵ. Introducing the previous expansions in the Eq. (50), applying Taylor expansion to $f_{\sigma(*)}$ yields:

$$
f_{\sigma(*)} = f^{(0)}_{\sigma(*)} + \epsilon f^{(1)}_{\sigma(*)} + \epsilon^2 f^{(2)}_{\sigma(*)} + \cdots , \tag{57}
$$

where $f^{(k)}_{\sigma(*)}$ $(k = 1, 2, \cdots)$ are known polynomial functions of the moments. Corresponding to Eq. (45), the coefficients in all these expansions are assumed to satisfy

$$\frac{\partial f^{(m)}}{\partial \alpha} = O(1), \qquad \frac{\partial M^{(m)}}{\partial \alpha} = O(1), \tag{58}$$

where $f^{(m)} = f^{(m)}_{\sigma(*)}, f^{(m)}_{\sigma}$, $\alpha = t, x_i$ and $M = \rho_\sigma, q_{\sigma i}$.

> (!!) The previous expansions cannot be applied directly to Eq. (52) because the latter involves the solution in different neighboring points.

Before substituting the above expansions into Eq. (52) and equating the terms of the same order of power of ϵ, we have to express $f_\sigma(t+\epsilon^2, x_i, V_i)$, $f_\sigma(t, x_i - V_i\epsilon, V_i)$, and $g_\sigma(t, x_i - V_i\epsilon, V_i)$ as their Taylor expansions around (t, x_i)

$$f_\sigma(t + \epsilon^2, x_i, V_i) = \sum_{k=0}^{\infty} \frac{\epsilon^{2k}}{k!}\, \partial t^k\, f_\sigma(t, x_i, V_i), \tag{59}$$

$$f_\sigma(t, x_i - V_i\epsilon, V_i) = \sum_{k=0}^{\infty} \frac{(-\epsilon)^k}{k!}\, \partial_S^k\, f_\sigma(t, x_i, V_i), \tag{60}$$

$$g_\sigma(t, x_i - V_i\epsilon, V_i) = \sum_{k=0}^{\infty} \frac{(-\epsilon)^k}{k!}\, \partial_S^k\, g_\sigma(t, x_i, V_i), \tag{61}$$

where $\partial_S = V_1\partial_{x_1} + V_2\partial_{x_2}$. Introducing the previous Taylor expansions in Eq. (52) and then consequently the expansion given by Eq. (54) yields the expressions for the coefficients $f^{(k)}_\sigma$ $(k = 1, 2, \cdots)$ as follows.

$$f^{(k)}_\sigma = f^{(k)}_{\sigma(*)} - g^{(k)}_\sigma, \tag{62}$$

$$g^{(0)}_\sigma = 0, \tag{63}$$

$$g^{(1)}_\sigma = \tau_\sigma \partial_S f^{(0)}_{\sigma(*)}, \tag{64}$$

$$g^{(2)}_\sigma = \tau_\sigma[\partial_t f^{(0)}_{\sigma(*)} + \partial_S f^{(1)}_{\sigma(*)} - \omega_\sigma \partial^2_S f^{(0)}_{\sigma(*)}], \tag{65}$$

where

$$\omega_\sigma = \tau_\sigma - 1/2. \tag{66}$$

Clearly the discrete effects due to the low accuracy of the forward Euler integration rule is shown by the fact that $\omega_\sigma \neq \tau_\sigma$, as it should be for the continuous model. Multiplying Eq. (64) by the lattice velocity and summing over all the lattice velocities yields

$$\lambda_\sigma \rho^{(0)}_\sigma [\boldsymbol{u}^{*(1)}_\sigma - \boldsymbol{u}^{(1)}_\sigma] = \nabla p^{(0)}_\sigma \tag{67}$$

where $p^{(0)}_\sigma = \varphi_\sigma/3\, \rho^{(0)}_\sigma$. The previous expression can be recasted as

$$\lambda_\sigma \rho^{(0)} \sum_\varsigma \frac{m^2}{m_\sigma m_\varsigma} \frac{B_{\sigma\varsigma}}{B_{\sigma\sigma}}\, x_\sigma x_\varsigma [\boldsymbol{u}^{(1)}_\varsigma - \boldsymbol{u}^{(1)}_\sigma] = \nabla p^{(0)}_\sigma, \tag{68}$$

or equivalently

$$\nabla p_\sigma^{(0)} = p^{(0)} \sum_\varsigma B_{\sigma\varsigma}\, y_\sigma y_\varsigma [\boldsymbol{u}_\varsigma^{(1)} - \boldsymbol{u}_\sigma^{(1)}], \tag{69}$$

which it is perfectly equivalent to the Maxwell-Stefan model.

Summing Eq. (65) over all the lattice velocities yields

$$\partial_t \rho_\sigma^{(0)} + \boldsymbol{\nabla} \cdot [\rho_\sigma^{(0)} \boldsymbol{u}_\sigma^{*(1)}] = \omega_\sigma \nabla^2 p_\sigma^{(0)}, \tag{70}$$

or equivalently

$$\partial_t \rho_\sigma^{(0)} + \boldsymbol{\nabla} \cdot [\rho_\sigma^{(0)} \boldsymbol{u}_\sigma^{(1)}] = \omega_\sigma \nabla^2 p_\sigma^{(0)} - \boldsymbol{\nabla} \cdot [\rho_\sigma^{(0)} \boldsymbol{u}_\sigma^{*(1)} - \rho_\sigma^{(0)} \boldsymbol{u}_\sigma^{(1)}], \tag{71}$$

and

$$\partial_t \rho_\sigma^{(0)} + \boldsymbol{\nabla} \cdot [\rho_\sigma^{(0)} \boldsymbol{u}_\sigma^{(1)}] = (\omega_\sigma - \tau_\sigma) \nabla^2 p_\sigma^{(0)} = -1/2 \nabla^2 p_\sigma^{(0)} \neq 0. \tag{72}$$

The simple BGK scheme does not preserve the mass continuity for the single species. Cearly this is due to the low accuracy of the forward Euler integration rule.

> (!!) This is indeed bad news, but the problem can be easily solved by considering a multiple-relaxation-time (MRT) scheme, because, in this case, the single species continuity is forced by the collision matrix.

4.3 Efficient numerical implementation

It is well known that it is very convenient to discretize the LBM schemes along the characteristics, i.e. along the lattice velocities, because they are constant and analytical known. However, as discussed in the previous section, the popular forward Euler integration rule can not be applied in this case because it leads to a lack of mass conservation [32]. Consequently a more accurate scheme must be considered: for example, the second-order Crank–Nicolson rule is enough in order to avoid this problem.

Let us discretize Eq. (46) by the following formula

$$f_\sigma^+ = f_\sigma + (1-\theta)\, \lambda_\sigma \left[f_{\sigma(*)} - f_\sigma \right] + \theta\, \lambda_\sigma^+ \left[f_{\sigma(*)}^+ - f_\sigma^+ \right], \tag{73}$$

where the argument (t, x_i) is omitted and the functions computed in $(t + \epsilon^2, x_i + \epsilon\, V_i)$ are identified by the superscript $+$. The Crank–Nicolson rule is recovered for $\theta = 1/2$. The previous formula would force one to consider quite complicated integration procedures [32]. Fortunately a simple variable transformation has been already proposed in order to simplify this task [33], and successfully applied in case of mixtures [34]. The generalization of this procedure to the MRT formulation for mixtures is trivial by following Ref. [35].

Let us introduce a local transformation

$$g_\sigma = f_\sigma - \theta\, \lambda_\sigma \left[f_{\sigma(*)} - f_\sigma \right]. \tag{74}$$

Substituting the transformation given by Eq. (74) into Eq. (73) yields

$$g_\sigma^+ = g_\sigma + \frac{\lambda_\sigma}{1 + \theta \lambda_\sigma} \left[f_{\sigma(*)} - g_\sigma \right], \tag{75}$$

where it is worth the effort to remark that the local equilibrium remains unchanged. Essentially the algorithm consisists of (a) appling the previous transformation $f_\sigma \to g_\sigma$ defined by Eq. (74), then (b) computing the collision step $g_\sigma \to g_\sigma^+$ by means of the formula given by Eq. (75) and finally (c) coming back to the original discrete distribution function $g_\sigma^+ \to f_\sigma^+$. The problem, in case of mixtures, arises from the last step. In fact, the formula required in order to perform the last task (c) is

$$f_\sigma^+ = \frac{g_\sigma^+ + \theta\,\lambda_\sigma^+ f_{\sigma(*)}^+}{1 + \theta\,\lambda_\sigma^+}. \tag{76}$$

In order to compute both λ_σ^+ (depending on total pressure and total density) and $f_{\sigma(*)}^+$, the updated hydrodynamic moments, i.e. the hydrodynamic moments at the new time step, are required. Since the single component density is conserved, recalling Eq. (74) yields

$$\rho_\sigma^+ = \langle g_\sigma^+ \rangle, \tag{77}$$

consequently it is possible to compute p_σ^+, ρ^+, p^+ and finally λ_σ^+.

However this is not the case for the single component momentum, because this is not a conserved quantity and hence the first order moments for g_σ^+ and f_σ^+ differ [34]. Recalling Eq. (74) and taking the first order moment of it yields

$$\langle V_i\, g_\sigma^+ \rangle = \rho_\sigma^+ u_{\sigma i}^+ - \theta\,\lambda_\sigma^+ \rho_\sigma^+ (u_{\sigma i}^{*+} - u_{\sigma i}^+) = \rho_\sigma^+ u_{\sigma i}^+ - \theta\, p^+ \sum_\varsigma B_{\sigma\varsigma}\, y_\sigma^+ y_\varsigma^+ (u_{\varsigma i}^+ - u_{\sigma i}^+). \tag{78}$$

It is worth the effort to point out an important property. Summing the previous equations for all the components yields

$$\sum_\sigma \langle V_i\, g_\sigma^+ \rangle = \rho^+ u_i^+, \tag{79}$$

which means that, since the total mixture momentum is conserved, then it is possible to compute it directly by means of g_σ^+. For this reason, it is possible to consider a simplified procedure in case of particles with similar masses.

4.3.1 Particles with similar masses

In case of particles with similar masses, $u_{\sigma i}^{*+} \cong u_i^+$ and Eq. (78) reduces to

$$\langle V_i\, g_\sigma^+ \rangle \cong \rho_\sigma^+ u_{\sigma i}^+ - \theta\,\lambda_\sigma^+ \rho_\sigma^+ (u_i^+ - u_{\sigma i}^+), \tag{80}$$

and equivalently, by taking into account Eq. (79),

$$\rho_\sigma^+ u_{\sigma i}^+ \cong \frac{\langle V_i\, g_\sigma^+ \rangle + \theta\,\lambda_\sigma^+ x_\sigma^+ \sum_\sigma \langle V_i\, g_\sigma^+ \rangle}{1 + \theta\,\lambda_\sigma^+}. \tag{81}$$

Actually the situation is even simpler, bacause the previous formula is not needed. In fact, if $u_{\sigma i}^{*+} \cong u_i^+$, it is enough u_i^+ by Eq. (79) to compute $f_{\sigma(*)}^+$ for the back transformation given by Eq. (76).

4.3.2 Particles with different masses

In the general case, Eq. (78) can be recasted as

$$\langle V_i\, g_\sigma^+ \rangle = q_{\sigma i}^+ - \theta\, \lambda_\sigma^+ \sum_\varsigma \chi_{\sigma\varsigma}\, (x_\sigma^+ q_{\varsigma i}^+ - x_\varsigma^+ q_{\sigma i}^+), \tag{82}$$

where $q_{\sigma i}^+ = \rho_\sigma^+ u_{\sigma i}^+$ and

$$\chi_{\sigma\varsigma} = \frac{m^2}{m_\sigma m_\varsigma} \frac{B_{\sigma\varsigma}}{B_{\sigma\sigma}}. \tag{83}$$

Finally, grouping together common terms yields

$$\langle V_i\, g_\sigma^+ \rangle = \left[1 + \theta\, \lambda_\sigma^+ \sum_\varsigma (\chi_{\sigma\varsigma}\, x_\varsigma^+) \right] q_{\sigma i}^+ - \theta\, \lambda_\sigma^+\, x_\sigma^+ \sum_\varsigma (\chi_{\sigma\varsigma}\, q_{\varsigma i}^+). \tag{84}$$

Clearly the previous expression defines a liner system of algebraic equations for the unknowns $q_{\sigma i}^+$. This means that in order to compute the updated values for all $q_{\sigma i}^+$ a linear system of equations must be solved in terms of known quantities $\langle V_i\, g_\sigma^+ \rangle$. Obviously the solvability condition for the previous system depends on the updated mass concentrations and it can not be ensured in general. Note that this potential restriction of the discussed scheme is a constraint of the proposed numerical implementation and not of the kinetic model itself. The possibility to tune θ is not available, because all the schemes for $\theta \neq 1/2$ may imply a lack of mass conservation. Even though this feature did not represent a problem in the reported numerical simulations, it should be further investigated.

In the degenerate case $\chi_{\sigma\varsigma} = 1$, i.e. particles with equal masses, Eq. (84) reduces to

$$\langle V_i\, g_\sigma^+ \rangle = \left(1 + \theta\, \lambda_\sigma^+\right)\, q_{\sigma i}^+ - \theta\, \lambda_\sigma^+\, x_\sigma^+ q_i^+, \tag{85}$$

which is equivalent to Eq. (81).

In the next section, the results for some numerical simulations are reported.

5 Numerical examples

5.1 Simple code

In order to simplify the understanding this lecture, an example code has been prepared. The source code can be *freely downloaded* at

(!!) *http://staff.polito.it/pietro.asinari/rome08/*

5.2 Fickian limiting test cases

In this notes, some simple numerical examples are considered, essentially concerning the recovered macroscopic diffusion model in the continuum limit. In particular, the Maxwell–Stefan diffusion model, in comparison with the simpler Fick model, allows one to automatically recover the effective diffusion coefficients in different limiting cases, depending on the

local concentrations, without any *a priori* guess about the concentration fields. In particular, in the reported numerical simulations, this feature will be verified in two limiting cases: (a) the solvent test case and (b) the dilute test case [36, 1]. The geometrical configuration and the procedure in order to measure the transport coefficients is quite standard [37, 38] and it can be physically explained as the mixing in an opposed-jet configuration [34].

In case of ternary mixture Eq. (16) reduces to

$$n\nabla y_1 = B_{12}y_1\boldsymbol{k}_2 + B_{13}y_1\boldsymbol{k}_3 - (B_{12}y_2 + B_{13}y_3)\boldsymbol{k}_1, \tag{86}$$

$$n\nabla y_2 = B_{21}y_2\boldsymbol{k}_1 + B_{23}y_2\boldsymbol{k}_3 - (B_{21}y_1 + B_{23}y_3)\boldsymbol{k}_2, \tag{87}$$

$$n\nabla y_3 = B_{31}y_3\boldsymbol{k}_1 + B_{32}y_3\boldsymbol{k}_2 - (B_{31}y_1 + B_{32}y_2)\boldsymbol{k}_3. \tag{88}$$

Let us consider a 1D computational domain, filled by a ternary mixture. All the physical quantities will be expressed in lattice units. The molecular weights are $m_\sigma = [1, 2, 3]$ and consequently the corrective factors are $\varphi_\sigma = [1, 1/2, 1/3]$. The theoretical Fick diffusion coefficient is $D_\sigma = \alpha/m_\sigma$, where $\alpha \in [0.002, 0.8]$ and the theoretical Maxwell–Stefan diffusion resistance is given by

$$B_{\sigma\varsigma} = \beta \left(\frac{1}{m_\sigma} + \frac{1}{m_\varsigma}\right)^{-1/2}, \tag{89}$$

where $\beta \in [5, 166]$.

The computational domain is defined by $(t, x) \in [0, T] \times [0, L]$. The boundary conditions for all the components at the borders of the computational domain, i.e. at $x = 0, L$, are of Neumann type, i.e. $\partial p_\sigma/\partial x = 0$ at any time. The initial conditions depends on the considered limiting case (see below). The spatial discretization step is called δx and the total number of grid points is $N_x = L/\delta x = 100$. Similarly the time discretization step is selected in such a way that $\delta t \sim \delta x$ in order to have $c = \delta x/\delta t = 1$, and in particular $N_t = T/\delta t = 30$.

5.2.1 Solvent test case

A component of a mixture is called *solvent* if its concentration is predominant in comparison with the other components of the mixture. Let us suppose that, in our ternary mixture, the component 3 is a solvent. In particular, the initial conditions for the solvent test case are given by

$$p_1(0, x) = \Delta p \left[1 + \tanh\left(\frac{x - L/2}{\delta x}\right)\right] + p_s, \tag{90}$$

$$p_2(0, x) = \Delta p \left[1 - \tanh\left(\frac{x - L/2}{\delta x}\right)\right] + p_s, \tag{91}$$

$$p_3(0, x) = 1 - 2\,(\Delta p + p_s), \tag{92}$$

where clearly $p(0, x) = \sum_\sigma p_\sigma = 1$. In the reported numerical simulations, $\Delta p = p_s = 0.01$. The parameter p_s is a small pressure shift in order to avoid divisions by zero in passing from the momentum to the velocity.

Hence $y_3 \cong 1$ and consequently $y_1 \cong 0$ and $y_2 \cong 0$. Under these assumptions, Eqs. (86, 87) reduce to

$$\nabla y_1 = -B_{13} y_1 (u_1 - v) = B_{13} y_1 (v - u_1), \tag{93}$$

$$\nabla y_2 = -B_{23} y_2 (u_2 - v) = B_{23} y_2 (v - u_2), \tag{94}$$

Consequently the measured diffusion resistances are given by

$$B_{13}^* = \frac{1}{D_1^*} = \frac{\partial y_1 / \partial x}{y_1 (v - u_1)}, \tag{95}$$

$$B_{23}^* = \frac{1}{D_2^*} = \frac{\partial y_2 / \partial x}{y_2 (v - u_2)}, \tag{96}$$

where, since in this test, the Maxwell–Stefan model reduces to the Fick model, it is possible to define two Fick diffusion coefficients $D_1 = 1/B_{13}$ and $D_2 = 1/B_{23}$ for non-solvent components. Since the main attention was for the mass diffusion process, in the reported numerical results the single–relaxation–time (SRT) formulation was considered. For this reason, the viscous dynamics (next approximation of the mixture momentum equation) is not reliable. In particular, the SRT formulation does not allow one to relax all the single component stress tensors with the same mixture viscosity as it should be for recovering the mixture dynamics (see previous section on MRT formulation). This means that, for the reported simulations, the ratio between the Fick diffusion coefficient and the mixture viscosity $Sc = \nu / D$, i.e. the Schmidt number, is not reliable.

First of all, a generalized Fick model was implemented and the corresponding numerical results are reported in Figs. 3 and 4 for non-solvent component 1 and 2 respectively. In case of the Fick model, a direct correlation exists between the Fick diffusion coefficient and the relaxation frequency, namely $\lambda_\sigma = \varphi_\sigma / (3\, D_\sigma)$, and this explains the auxiliary axises of the previous figures. The implicit numerical implementation allows one to consider large relaxation frequencies, since the stability region is widened. The LBM implementation of the generalized Fick model well matches the expected transport coefficients. At the lowest and the highest end of the considered range, the measured transport coefficients slightly overestimate and underestimate the theoretical values respectively.

Secondly, a complete Maxwell–Stefan model, without *a priori* restriction of the mixture-averaged approximation [39, 36], was implemented and the corresponding numerical results are reported in Figs. 5 and 6 respectively. The key idea is to verify that the model automatically reduces to the solvent limit, i.e. that the dynamics of component 1 is mainly ruled by resistance B_{13} and that of component 2 by resistance B_{23}. In this case, there is no direct correlation between the Maxwell–Stefan resistances (three as the possible interacting couples) and the relaxation frequencies (three as the number of components). As the number of components increases, then the number of Maxwell–Stefan resistances is usually larger than the number of components. Also in this case, the LBM implementation of the Maxwell–Stefan model well matches the expected resistance coefficients.

5.2.2 Dilute test case

A component of a mixture is said *dilute* if its concentration is negligible in comparison with the other components of the mixture. Let us suppose that, in our ternary mixture, the

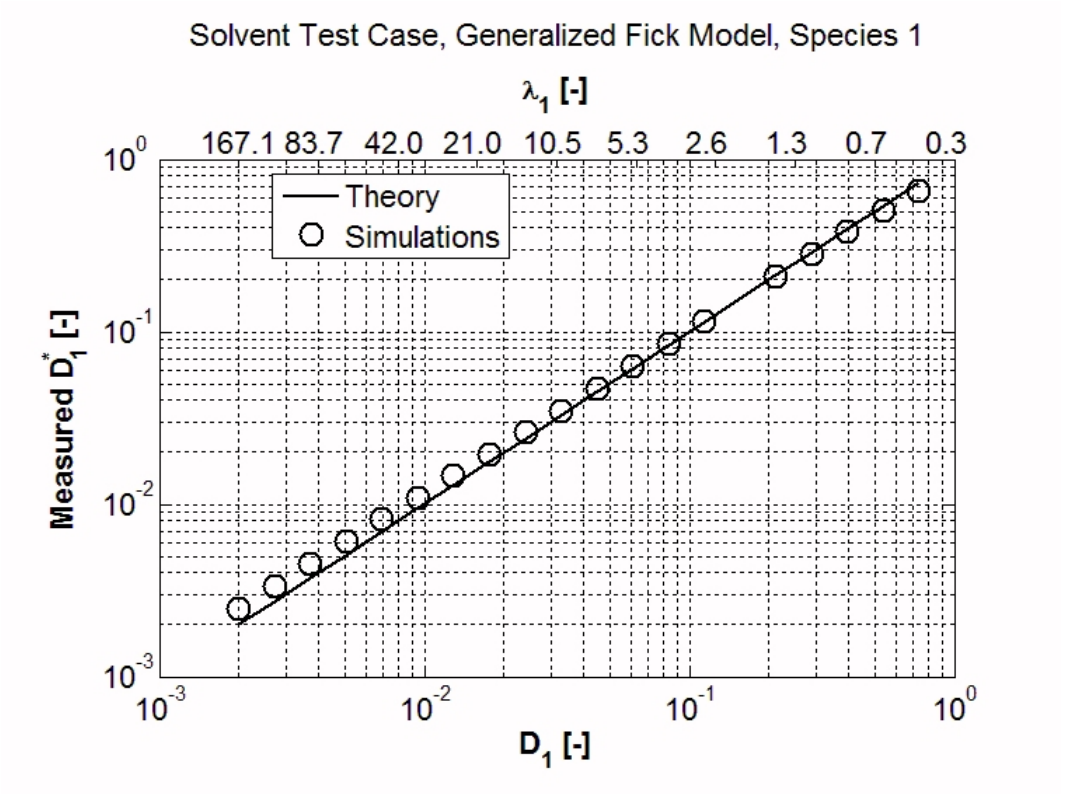

Figure 3: Solvent test case for a ternary mixture: $y_3 \cong 1$ and consequently $y_1 \cong 0$ and $y_2 \cong 0$. Comparison between expected Fick diffusion coefficient for component 1, i.e. D_1, with the transport coefficient D_1^* from the numerical implementation of the generalized Fick model, measured by Eq. (95). The corresponding values for the relaxation frequencies λ_1 are reported as well.

component 1 is dilute. In particular, the initial conditions for the dilute test case are given by

$$p_1(0,x) = \Delta p \left[1 + \tanh\left(\frac{x - L/2}{\delta x}\right)\right] + p_s, \tag{97}$$

$$p_2(0,x) = \Delta p \left[1 - \tanh\left(\frac{x - L/2}{\delta x}\right)\right] + p_s + (1-r)\,(1 - 2\,\Delta p), \tag{98}$$

$$p_3(0,x) = r\,(1 - 2\,\Delta p) - 2\,p_s, \tag{99}$$

where clearly $p(0,x) = \sum_\sigma p_\sigma = 1$. In the reported numerical simulations, $\Delta p = p_s = 0.01$ and $r = 1/2$. Clearly r must be close to $1/2$, otherwise this test case reduces to the previous one about existence of a solvent. Again the parameter p_s is a small pressure shift in order to avoid divisions by zero in passing from the momentum to the velocity.

Hence $y_1 \cong 0$ and consequently $y_1 \ll y_2 + y_3$. Under these assumptions, Eq. (86) reduces to

$$\nabla y_1 = -(B_{12} y_2 + B_{13} y_3)\boldsymbol{k}_1 = y_1\, B_1\,(v - u_1), \tag{100}$$

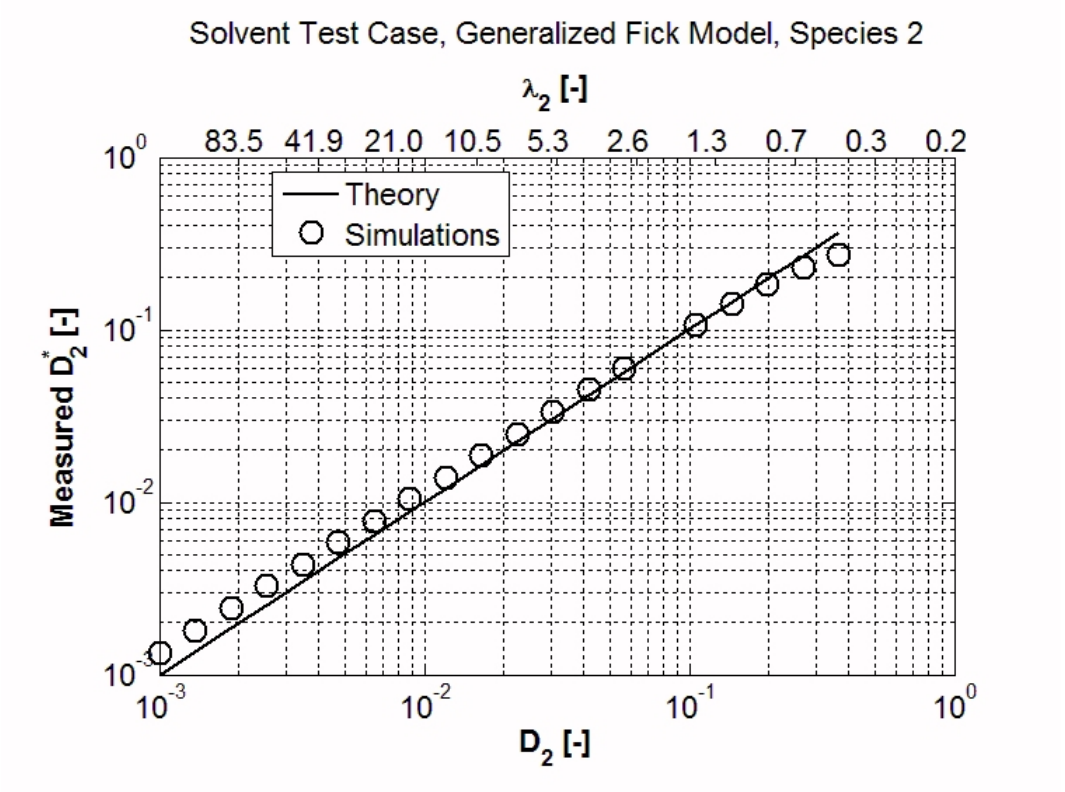

Figure 4: Solvent test case for a ternary mixture: $y_3 \cong 1$ and consequently $y_1 \cong 0$ and $y_2 \cong 0$. Comparison between expected Fick diffusion coefficient for component 2, i.e. D_2, with the transport coefficient D_2^* from the numerical implementation of the generalized Fick model, measured by Eq. (96). The corresponding values for the relaxation frequencies λ_2 are reported as well.

where $B_1 = B_{12}y_2 + B_{13}y_3$ is an equivalent effective resistance. Consequently the measured diffusion resistance is given by

$$B_1^* = \frac{1}{D_1^*} = \frac{\partial y_1/\partial x}{y_1(v - u_1)}, \tag{101}$$

where, since also in this test, the Maxwell–Stefan model reduces to the Fick model, it is possible to define a Fick diffusion coefficients $D_1 = 1/B_1$ for the dilute component. Concerning the actual Schmidt number, considerations similar to those already discussed for the previous test case holds here as well.

In Fig. 7, the numerical results for the Maxwell–Stefan implementation are reported and, in particular, the measured values for the equivalent effective resistance B_1 are compared with the theoretical expected values. Also in this case, the LBM implementation of the Maxwell–Stefan model well matches the expected values. It is worth the effort to point out that the effective resistance B_1 is never directly imposed in the code, but it is a natural outcome of the model, which depends on the local molar concentrations.

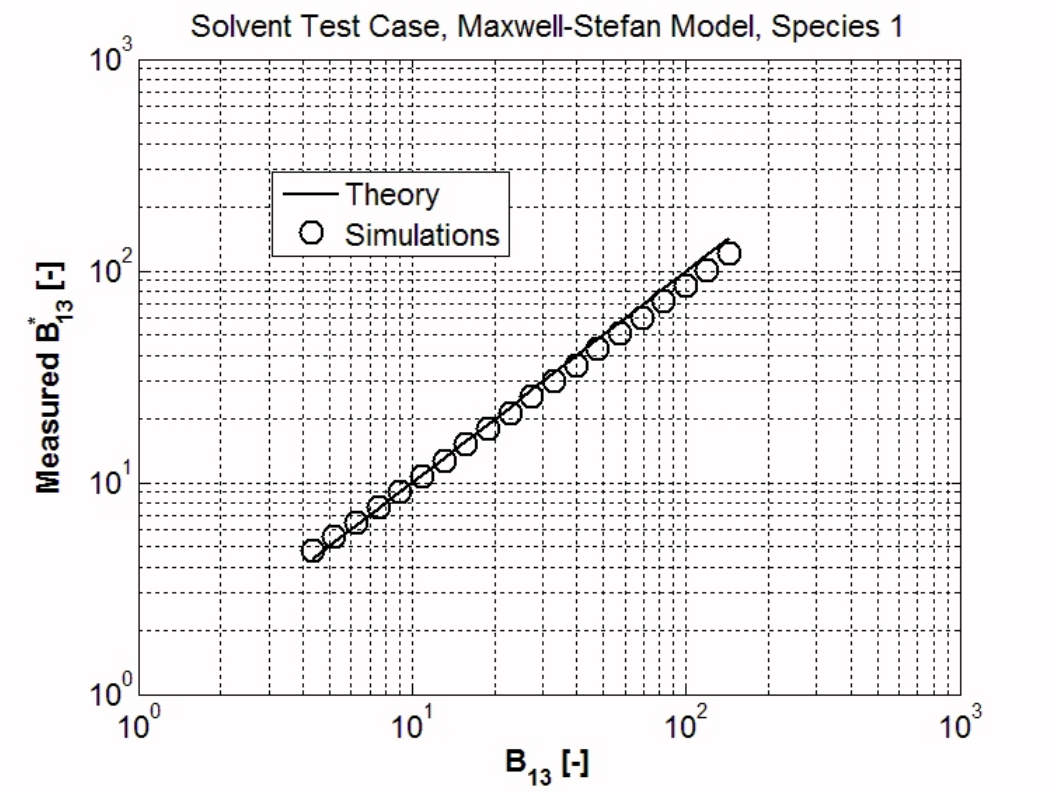

Figure 5: Solvent test case for a ternary mixture: $y_3 \cong 1$ and consequently $y_1 \cong 0$ and $y_2 \cong 0$. Comparison between expected Maxwell–Stefan resistance coefficient for component 1, i.e. B_{13}, with the resistance coefficient B^*_{13} from the numerical implementation of the Maxwell–Stefan model, measured by Eq. (95).

5.3 Non-Fickian test case: Stefan tube

The previous numerical simulations proved that the proposed model allows one to recover some well-known results for Fickian test cases. Since there are already plenty of lattice Boltzmann implementations that simulate Fickian diffusion, the innovative part of the previous simulations relies on the fact that all the transport coefficients of the model are kept constant for all the tests, without introducing any artificial external tuning, in order to match the considered limiting test case.

In this section, the full capabilities of the Maxwell–Stefan model will be proved for a non-Fickian test case. Let us consider a popular test, i.e. the Stefan tube (see chapter 2 of [2] for details). The Stefan tube is a simple device sometimes used for measuring diffusion coefficients in binary vapor mixtures, in case of the presence of an additional gas carrier. It is essentially a vertical tube, open at one end, where the carrier flow licks orthogonally the tube opening. In the bottom of the tube is a pool of quiescent liquid. The vapor that evaporates from this pool diffuses to the top of the tube. The stream of gas carrier across the top of the tube keeps the molar concentration of diffusing vapor there essentially to nothing. The molar concentration of the vapor at the vapor-liquid interface is its equilibrium value.

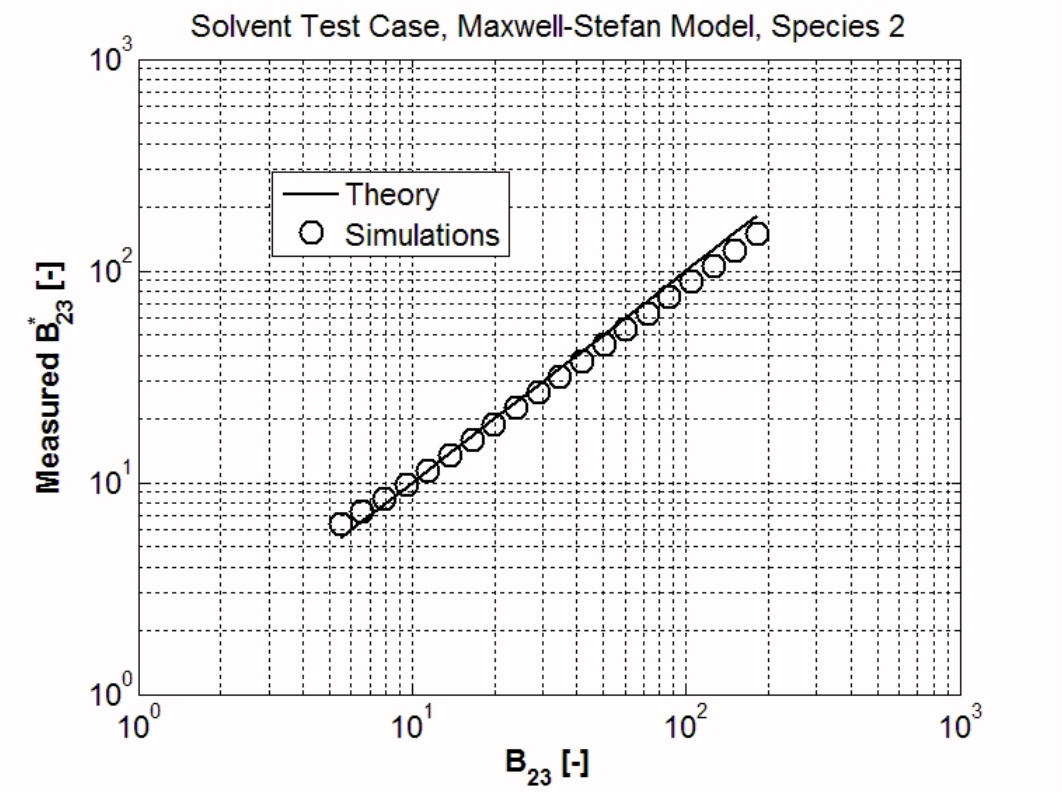

Figure 6: Solvent test case for a ternary mixture: $y_3 \cong 1$ and consequently $y_1 \cong 0$ and $y_2 \cong 0$. Comparison between expected Maxwell–Stefan resistance coefficient for component 2, i.e. B_{23}, with the resistance coefficient B^*_{23} from the numerical implementation of the Maxwell–Stefan model, measured by Eq. (96).

For sake of simplicity, let us consider the same ternary mixture, already discussed in the previous sections, where the third species is assumed to be the gas carrier. Let us assume Eq. (89) for the Maxwell–Stefan diffusion resistance, with $\beta = 66.13$, which implies $B_{13} = 57.27$, $B_{12} = 54.00$, $B_{23} = 72.44$.

The computational domain is defined by $(t, x) \in [0, T] \times [0, L]$. Concerning the boundary conditions, the partial pressures for all the species at the bottom of the tube $p_1(0, 0) = 0.319$, $p_2(0, 0) = 0.528$, $p_3(0, 0) = 0.1530$ and those at the opening of the tube $p_1(0, L) = 0.0$, $p_2(0, L) = 0.0$, $p_3(0, L) = 1.0$ are specified. In particular, the pressure condition proposed in Ref. [40] was adopted. This boundary condition is now available for the lattice Boltzmann method too [41]. Recasting this condition for the compressible case reads

$$-p_\sigma \boldsymbol{n} + \nu \frac{\partial(\rho_\sigma \boldsymbol{u}_\sigma)}{\partial \boldsymbol{n}} = -\tilde{p}_\sigma \boldsymbol{n}, \tag{102}$$

where $\boldsymbol{n}$ is the unit outer normal direction at the boundary, p_σ is the pressure at the boundary and $\tilde{p}_\sigma$ is the average pressure at the boundary. In our mono-dimensional test case, clearly $\tilde{p}_\sigma = p_\sigma$ and the previous condition implies $\partial(\rho_\sigma u_{\sigma\,1})/\partial x = 0$ at both $x = 0, L$. This means

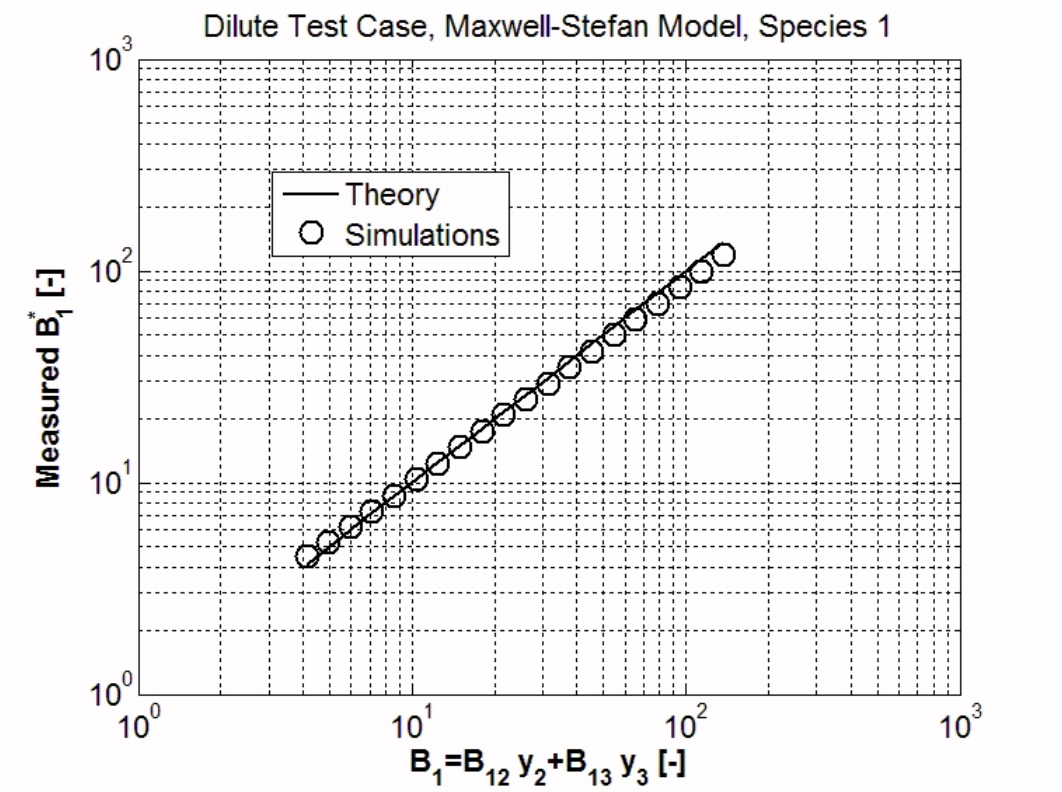

Figure 7: Dilute test case for a ternary mixture: $y_1 \cong 0$ and consequently $y_1 \ll y_2 + y_3$. Comparison between expected Maxwell–Stefan equivalent effective resistance for component 1, i.e. B_1, with the resistance coefficient B_1^* from the numerical implementation of the Maxwell–Stefan model, measured by Eq. (101).

that we have to consider both Dirichlet boundary conditions (for partial pressures) and homogeneous Neumann boundary conditions (for single species momenta).

The initial conditions are

$$p_1(0,x) = p_1(0,0)\,\frac{1}{2}\left[1-\tanh\left(\frac{x-L/2}{\delta x}\right)\right]+p_s, \tag{103}$$

$$p_2(0,x) = p_2(0,0)\,\frac{1}{2}\left[1-\tanh\left(\frac{x-L/2}{\delta x}\right)\right]+p_s, \tag{104}$$

$$p_3(0,x) = [1-p_3(0,0)]\,\frac{1}{2}\left[1+\tanh\left(\frac{x-L/2}{\delta x}\right)\right]+p_3(0,0), \tag{105}$$

where the constant $p_s = 10^{-4}$ has been introduced for stability reasons, i.e. for avoiding to divide per zero in the computation of the velocity.

The spatial discretization step is called δx and the total number of grid points is $N_x = L/\delta x = 60$. Similarly the time discretization step is selected in such a way that $\delta t \sim \delta x$ in order to have $c = \delta x/\delta t = 1$, and in particular $N_t = T/\delta t = 120,000$.

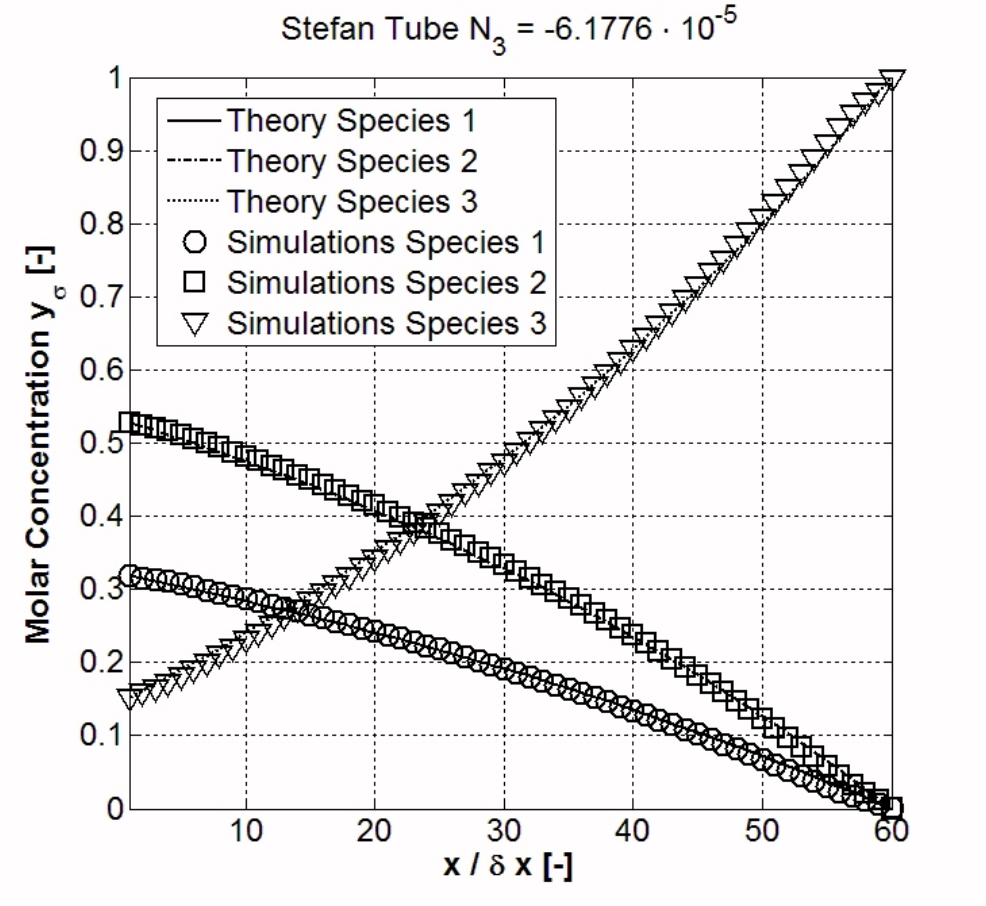

Figure 8: Non-Fickian test case: composition profiles in a Stefan diffusion tube. Negative flux is assumed for the gas carrier pointing toward the liquid bottom ($x = 0$), i.e. $N_3 = -6.1776 \cdot 10^{-5}$. The reference solutions are obtained by solving the boundary value problem by the shooting method and a multi-variable Newton method.

Concerning the numerical solution, at constant temperature and pressure, the total molar density is constant and the driving forces are the molar concentration gradients ∇y_σ. Furthermore, since there are no radial or circumferential gradients in the composition, the continuity equation at steady state implies that $\rho_\sigma u_{\sigma\,1}$ is a constant, as well as $N_\sigma = y_\sigma u_{\sigma\,1}$. The first two Eqs. (86, 87) can be rewritten as

$$\frac{dy_1}{dx} = B_{12}(y_1 N_2 - y_2 N_1) + B_{13}[y_1 N_3 - (1 - y_1 - y_2)N_1], \tag{106}$$

$$\frac{dy_2}{dx} = B_{12}(y_2 N_1 - y_1 N_2) + B_{23}[y_2 N_3 - (1 - y_1 - y_2)N_2], \tag{107}$$

while Eq. (88) can be omitted, since it is not linearly independent on the previous ones. The previous system of ordinary differential equations, with the boundary conditions already discussed, realizes a boundary value problem, which can be solved, for example, by the

shooting method [42]. Essentially the idea is to define the proper values for the parameters N_1, N_2, N_3 in order to ensure the required boundary conditions at $x = L$. The solution of this problem is not unique. In fact, some additional information concerning the physics of the problem needs to be provided. For example, from the practical point of view, usually the gas carrier does not dissolve in the liquid and, for this reason, its flux is zero, i.e. $N_3 = 0$. In general, the pressure difference across the tube of the gas carrier is responsible of its dynamics. Hence the flux of the gas carrier points toward the liquid pool at the bottom, i.e. $N_3 \leq 0$. In the following, only the test with $N_3 = -6.1776 \cdot 10^{-5}$ is considered.

In Fig. 8 the molar concentration profiles are reported. The numerical simulations performed by the proposed LBM model agree well with the results obtained by directly solving the boundary value problem. Clearly the molar concentrations show a non-Fickian behavior. In fact, the Fick model would prescribe linear profiles of the molar concentrations for this boundary value problem. The coupling among the species, which is responsible of the non linear profiles, can not be simulated by any simplified Fick diffusion coefficient. This feature, which has been experimentally proved by Carty and Schrodt (1975) [4], demonstrates the superiority of the Maxwell–Stefan formulation.

Concerning the LBM implementation of the model, special attention must be devoted to the partial pressure boundary conditions in a general application. For the reported results, a simple boundary condition in the moment space was adopted, but more complicated cases would required more accurate boundary conditions, like those reported in Ref. [41].

Acknoledgements

The author would like to thank prof. Li-Shi Luo of Old Dominion University (USA) and prof. Taku Ohwada of Kyoto University (Japan) for many enlightening discussions concerning the kinetic equations for mixtures and the asymptotic analysis of kinetic equations respectively. Moreover he would like to thank dr. Ilya Karlin of ETH-Zurich (Switzerland) for pointing out the new results reported in Ref. [34].

References

[1] C.E. Brennen. *Fundamentals of Multiphase Flow*. Cambridge University Press, United Kingdom, 2005.

[2] R. Taylor and R. Krishna. *Multicomponent Mass Transfer*. John Wiley & Sons, New York, 1993.

[3] J. O. Hirschfelder, C. F. Curtiss, and R. B. Bird. *Molecular Theory of Gases and Liquids*. Wiley, New York, 1954.

[4] R. Krishna and J.A. Wesselingh. Maxwell-stefan approach to mass transfer. *Chemical Engineering Science*, 52(6):861–911, 1997.

[5] S. Chapman and T. G. Cowling. *The Mathematical Theory of Non-Uniform Gases*. Cambridge University Press, Cambridge, UK, 3rd edition, 1970.

[6] J. H. Ferziger and H. G. Kaper. *Mathematical Theory of Transport in Gases*. North Holland, Amsterdam, 1972.

[7] L. C. Woods. *An Introduction to the Kinetic Theory of Gases and Magnetoplasmas*. Oxford University Press, Oxford, UK, 3 edition, 1993.

[8] S. Harris. *An Introduction to the Theory of the Boltzmann Equation*. Dover, Mineola, NY, 2004.

[9] P. Andries, K. Aoki, and B. Perthame. A consistent BGK-type model for gas mixtures. *J. Stat. Phys.*, 106(5/6):993–1018, 2002.

[10] I. Kolodner. *On the application of the Boltzmann equations to the theory of gas mixtures*. Phd thesis, New York University, New York, 1950.

[11] L.-S. Luo and S. S. Girimaji. Lattice Boltzmann model for binary mixtures. *Phys. Rev. E*, 66:035301(R), 2002.

[12] C. F. Curtiss and J. O. Hirschfelder. Transport properties of multicomponent gas mixtures. *J. Chem. Phys.*, 17:550–555, 1949.

[13] E. P. Gross and M. Krook. Models for collision processes in gases: Small-amplitude oscillations of charged two-component systems. *Phys. Rev.*, 102:593–604, 1956.

[14] E. P. Gross and E. A. Jackson. Kinetic models and the linearized Boltzmann equation. *Phys. Fluids*, 2(4):432–441, 1959.

[15] L. Sirovich. Kinetic modelling of gas mixtures. *Phys. Fluids*, 5:908–918, 1962.

[16] T. F. Morse. Kinetic model equations for a gas mixture. *Phys. Fluids*, 7:2012–2013, 1964.

[17] B. B. Hamel. Kinetic models for binary mixtures. *Phys. Fluids*, 8:418–425, 1965.

[18] L. Sirovich. Mixtures of Maxwell molecules. *Phys. Fluids*, 9:2323–2326, 1966.

[19] B. B. Hamel. Two-fluid hydrodynamic equations for a neutral, disparate-mass, binary mixtures. *Phys. Fluids*, 9:12–22, 1966.

[20] S. Ziering and M. Sheinblatt. Kinetic theory of diffusion in rarefied gases. *Phys. Fluids*, 9:1674–1685, 1966.

[21] E. Goldman and L. Sirovich. Equations for gas mixtures. *Phys. Fluids*, 10:1928–1940, 1967.

[22] J. M. Greene. Improved Bhatnagar-Gross-Krook model of electron-ion collisions. *Phys. Fluids*, 16:2022–2023, 1973.

[23] H. Grad. Principles of the kinetic theory of gases. In S. Flügge, editor, *Handbuch der Physik*, pages 204–294. Springer, Berlin, 1958.

[24] J. C. Maxwell. On the dynamical theory of gases. *Philos. Trans. R. Soc.*, 157:26–78, 1866.

[25] P. L. Bhatnagar, E. P. Gross, and M. Krook. A model for collision processes in gases. I. Small amplitude processes in charged and neutral one-component systems. *Phys. Rev.*, 94:511–525, 1954.

[26] H. Grad. Theory of rarefied gases. In F. Devienne, editor, *Rarefied Gas Dynamics*, pages 100–138. Pergamon, London, 1960.

[27] P. Asinari. Viscous coupling based lattice Boltzmann model for binary mixtures. *Phys. Fluids*, 17(6):067102, 2005.

[28] V. Garzò, A. dos Santos, and J. J. Brey. A kinetic model for a multicomponent gas. *Phys. Fluids A*, 1(2):380–383, 1989.

[29] S. S. Chikatamarla, S. Ansumali, and I. V. Karlin. Entropic lattice Boltzmann models for hydrodynamics in three dimensions. *Phys. Rev. E*, 97(1):010201, 2006.

[30] W.-A. Yong and L.-S. Luo. Nonexistence of h theorems for the athermal lattice Boltzmann models with polynomial equilibria. *Phys. Rev. E*, 67:051105, 2003.

[31] Y. Sone. *Kinetic Theory and Fluid Dynamics*. Birkhäuser, Boston, 2nd edition, 2002.

[32] P. Asinari. Semi-implicit-linearized multiple-relaxation-time formulation of lattice Boltzmann schemes for mixture modeling. *Phys. Rev. E*, 73(5):056705, 2006.

[33] Z. L. Guo and T. S. Zhao. Explicit finite-difference lattice boltzmann method for curvilinear coordinates. *Phys. Rev. E*, 67:066709, 2003.

[34] S. Arcidiacono, I. V. Karlin, J. Mantzaras, and C. E. Frouzakis. Lattice boltzmann model for the simulation of the multicomponent mixtures. *Phys. Rev. E*, 76:046703–1—046703–11, 2007.

[35] A. Bardow, I.V. Karlin, and A.A. Gusev. General characteristic-based algorithm for off-lattice Boltzmann simulations. *Europhys. Lett.*, 75(3):434–440, 2006.

[36] W.E. Stewart R.B. Bird and E.N. Lightfoot. *Transport Phenomena*. John Wiley & Sons, New York, 1960.

[37] E. G. Flekkoy. Lattice Bhatnagar-Gross-Krook models for miscible fluids. *Phys. Rev. E*, 47:4247, 1993.

[38] M. E. McCracken and J. Abraham. Lattice Boltzmann methods for binary mixtures with different molecular weights. *Phys. Rev. E*, 71:046704, 2005.

[39] F. Williams. *Combustion Theory*. Benjamin/Cumming, California, 1986.

[40] R. Rannacher J. Heywood and S. Turek. Artificial boundaries and flux and pressure conditions for the incompressible navierstokes equations. *Int. J. Numer. Meth. Fluids*, 22:325–352, 1996.

[41] M. Junk and Z. Yang. Pressure boundary condition for the lattice boltzmann method. 2008. Submitted to Comput. Math. Appl.

[42] W.T. Vetterling W.H. Press, S.A. Teukolsky and B.P. Flannery. *Numerical Recipes 3rd Edition: The Art of Scientific Computing*. Cambridge University Press, Hong Kong, 2007.